THE EXTRACTION OF LANDSLIDES IN A SATELLITE IMAGE USING A DIGITAL ELEVATION MODEL

By

JOHN PATRICK DONAHUE

B.Sc., University of Massachusetts, 1983

A THESIS SUBMITTED IN PARTIAL FULFILMENT OF
THE REQUIREMENTS FOR THE DEGREE OF
MASTER OF APPLIED SCIENCE

in

THE FACULTY OF GRADUATE STUDIES
(Department of Forestry)

We accept this thesis as conforming
to the required standard

THE UNIVERSITY OF BRITISH COLUMBIA

September, 1987

In presenting this thesis in partial fulfilment of the requirements for an advanced degree at the University of British Columbia, I agree that the Library shall make it freely available for reference and study. I further agree that permission for extensive copying of this thesis for scholarly purposes may be granted by the head of my department or by his or her representatives. It is understood that copying or publication of this thesis for financial gain shall not be allowed without my written permission.

Department of Forestry

The University of British Columbia
1956 Main Mall
Vancouver, Canada
V6T 1Y3

Date October 5, 1987

ABSTRACT

Landslides in the landscape exhibit predictable properties of shape, structure and orientation. These properties are reflected to varying degrees in their depiction in a satellite image. Landslides can be isolated along with similar objects in a digital image using differential and template operators. Extraction of the landslide features from these images can proceed using a logic-based model which draws on an appropriate object definition approximating the depiction of the landslides in an edge-operated image and a digital elevation model.

An object extraction algorithm based on these concepts is used in repeated trials to ascertain the effectiveness of this automated approach. A low resolution linear object definition (Fischler et al., 1981) is used to isolate candidate pixel segments in three enhanced images. These segments are classified as landslides or non-landslides according to their image pixel intensity, length, slope, and orientation. Digital elevation data is used to evaluate slope and orientation criteria. Results are compared to an inventory of landslides made using aerial photographs.

Study results indicate that 17% to 28% of landslides in the image are identified for trials that produce a commission error rate of less than 50%. Commission errors are dominated by image objects related to roads and waste wood

areas in clearcuts. A higher rate of successful identification was noted for landslides which occurred within 15 years of image acquisition (24% to 32%), and was most apparent for the subset of that group which was located in areas that were harvested more than 15 years before acquisition or were unharvested (29% to 38%). Successful identifications in the trials are dominated by events greater than 300 metres long and wider than 20 metres. The results suggest that the approach is more reliable in unharvested areas of the image.

The poor quality of the digital elevation data, specifically artifacts produced by the contour-to-grid algorithm, was partly responsible for errors of commission and omission. The simplicity of the object definition used is another factor in error production. The methodology is not operational, but represents a realistic approach to scene segmentation for resource management given further refinement.

TABLE OF CONTENTS

I ABSTRACT ii
II TABLE OF CONTENTS iv
III LIST OF TABLES vi
VI LIST OF FIGURES vii
V ACKNOWLEDGMENTS ix

1. INTRODUCTION 1
   1.1 Landslide definition and process 2
   1.2 Literature review: landslide inventory 3
   1.3 Object extraction 6
      1.3.1 Literature review: linear object extraction 7
      1.3.2 A decision model for extraction of landslides 10
   1.4 Research objectives 12

2. MATERIALS AND METHODS 14
   2.1 Site description 14
   2.2 Baseline landslide inventory for the study site . 14
      2.2.1 Compilation 14
      2.2.2 Data adaptation 16
   2.3 Satellite imagery 19
      2.3.1 Image description 19
      2.3.2 Image band selection 19
      2.3.3 Edge detection 22
         2.3.3.1 Differential operator 22
         2.3.3.2 Template matching 24
         2.3.3.3 Threshold/template matching 28
   2.4 Digital topography 31

3. IMPLEMENTATION 39
   3.1 Introduction 39
   3.2 Image evaluation program 40
   3.3 Landslide image production and evaluation procedure 44

4. RESULTS AND DISCUSSION 50
   4.1 Results 50
      4.1.1 Commission errors 50
      4.1.2 Success characterisation 57
   4.2 Discussion 61
      4.2.1 Commission errors 68
      4.2.2 Identification successes and omissions 70
      4.2.3 Baseline inventory 72

5. CONCLUSIONS 74
   5.1 This study 74
   5.2 Research directions 76

6. LITERATURE CITED 78

7. GLOSSARY 82

8. APPENDIX A: Landslide detection in an enhanced satellite image 84
A.1 Procedure 84
A.2 Results and conclusions 85

9. APPENDIX B: Record of commission errors 89

10. APPENDIX C: Event characteristics and identification 92

11. APPENDIX D: Landslide template revision 110

LIST OF TABLES

3.1 Trial layout for landslide image production 46

4.1 Success and commission results for 14 trials 51

4.2(a,b) Causes of commission errors 58

4.3 Total number of events in each landslide category .. 62

4.4 Successful identifications for trial D 63

4.5 Successful identifications for trial M 64

4.6 Successful identifications for trial K 65

4.7 Successful identifications for trial N 66

4.8 Successful identifications for trial E 67

D.1 Success and commission results for study trials plus revised, eight direction template 112

LIST OF FIGURES

1.1 An example of a translational slide 4

1.2 Landsat TM image containing the study site 11

2.1 Location map of the study site 15

2.2 Results from three transects recorded across known landslide tracks 21

2.3 A demonstration of the Laplacian operator used in the study 24

2.4 The Laplacian edge image used in the study 25

2.5 The Duda Road Operator as presented by Fischler et al. (1981) 27

2.6 The landslide operator developed for the study 27

2.7 The landslide template image used in the study 27

2.8 Histogram of image band 3 of the study site 30

2.9a-d A portion of image band 3 of the study site thresholded at 4 pixel values 32

2.9e The threshold/template matching image used in the study 33

2.10 Synthetic view of the digital elevation model of the study site 34

2.11 The slope adjustment operator used to estimate point slope values from the digital elevation data 37

2.12 Code format for the fall line vector file 38

3.1 Pseudocode for segment identification 41

3.2 Pseudocode for segment length appraisal 42

3.3 Definitions for variables used in Figures 3.1 & 3.2 43

3.4 Histogram of Laplacian image 47

3.5 Histogram of template matching image 48

4.1 Trial D (Laplacian operator) 52

4.2 Trial M (Threshold/template operator) 53

4.3 Trial K (Template operator) 54

4.4 Trial N (Threshold/template operator) 55

4.5 Trial E (Laplacian operator) 56

4.6 Commission error A-4 59

4.7 Commission error B-16 60

A.1 Results: Detection rate of all landslide events for 3 thresholds of the Laplacian image 86

A.2 Results: Detection of landslide events by the Laplacian operator by landslide type 86

A.3 Part 1 results: Detection of landslide events by the Laplacian operator by landslide age 87

ACKNOWLEDGMENTS

I would like to thank my supervisor, Dr. Peter Murtha, and the members of my committee, especially Dr. Mark Sondheim, whose ongoing guidance and patience was invaluable. Mark's family was also quite kind to me on my frequent trips to Victoria for consultation. I also wish to recognise the able assistance of the technical staff at the Faculty of Forestry, namely Nedenia Krajci and Raoul Wiart, for their help and advice throughout. Tim Lee and Mark Majka, both with the Laboratory for Computational Vision, were extremely helpful with programming advice and software development. Finally, I want to thank Paula West for her remarkable patience and support during my tenure at UBC. This thesis was funded by the C.F.S. through the Faculty of Forestry Block Grant.

CHAPTER 1

INTRODUCTION

This thesis describes the application of image enhancement techniques and a digital elevation model (DEM) to an object detection and extraction problem in a satellite image. A methodology is proposed which utilises a logical approach to the aggregation of scene, object, and ancillary information, and a demonstration is presented which identifies landslide features in the image using this approach.

The extraction of landslides from a satellite image is an appropriate problem to investigate based on the need for an updatable inventory on forested lands, as well as an environmental monitoring system for water quality assessment. In Chapter One, a review of literature pertaining to the inventory of landslides on the landscape is supplemented by a review of automated object extraction techniques for extracting linear objects in digital images. The basis for the decision model is also discussed. Chapter Two describes the ground truth data for the study as well as the imagery, enhancement operations, and elevation data which will be employed in finding landslides. Chapter Three recounts the implementation of an automated system for extracting landslides from enhanced satellite images. Results are presented in Chapter 4. A discussion of the results from the methodology examines its success as compared to a conventional inventory, and possible reasons for the omission and commis-

sion errors encountered. Conclusions are made in Chapter 5, including some thoughts about future work.

Appendix A describes the procedure and results from a preliminary investigation into the use of a low resolution linear object definition (Fischler et al., 1981) to describe landslides in an enhanced satellite image. The results confirm the validity of such an approach, and helped to guide the design of the object extraction system employed in this thesis. Appendix B is a compilation of commission errors made in several trials of the methodology, and Appendix C is a catalogue of landslide event attributes and trial identification results. Appendix D explores the use of a landslide template which is slightly different than the one used in the study.

1.1 Landslide definition and process

"Landslide" is a generic term for several types of mass movements in the Coast Mountains of British Columbia and includes flows and slides (Varnes, 1958) as well as torrents (VanDine, 1985). It is used as such throughout this work.

The nomenclature indicates the process involved in a mass movement. A slide implies one or many shear failures along recognizable zones or planes. The rotational slide presents a concave surface, whereas the translational slide proceeds along a generally linear plane. A translational slide often takes on the narrow, linear shape of the classic mountain slope movement (Varnes, 1978:14). The rotational

slide, although commonly smaller, may give rise to larger, linear torrent events (VanDine, 1985). Figure 1.1 is an example of the track left by a translational slide which was initiated by a road sidecast failure. Flows are characterised by a viscous fluid motion and a lack of structural surfaces between the mass and the slope. According to Varnes, 'there is a complete gradation from debris slides to debris flows, depending on water content, mobility, and character of the movement'(1978:18). When such a flow occurs in a channel or gully, it is known as a debris torrent (Swanson and Swanston, 1977).

1.2 Literature review: landslide inventory

Methods for evaluating landslide hazard commonly require an inventory of slides which have occurred already in the area. Examples of these methods include those introduced by Sondheim and Rollerson (1985), Neilsen and Brabb (1978), Wieczorek (1984), and Howes (1987). An inventory may be used in combination with geologic information, or on its own in such schemes. Inventories are commonly drawn from evidence obtained from fieldwork, aerial photographs, and/or other remote sensing imagery. As such, the problem of identification of slope movement evidence in the landscape has been of interest to these and other workers.

Gresswell, Heller, and Swanston (1978) performed a predominately field-based inventory in support of their study in the Oregon Cascades. Methods for the identification

Figure 1.1. An example of a translational slide. Dimensions are approximately 200 metres long by 20 metres wide.

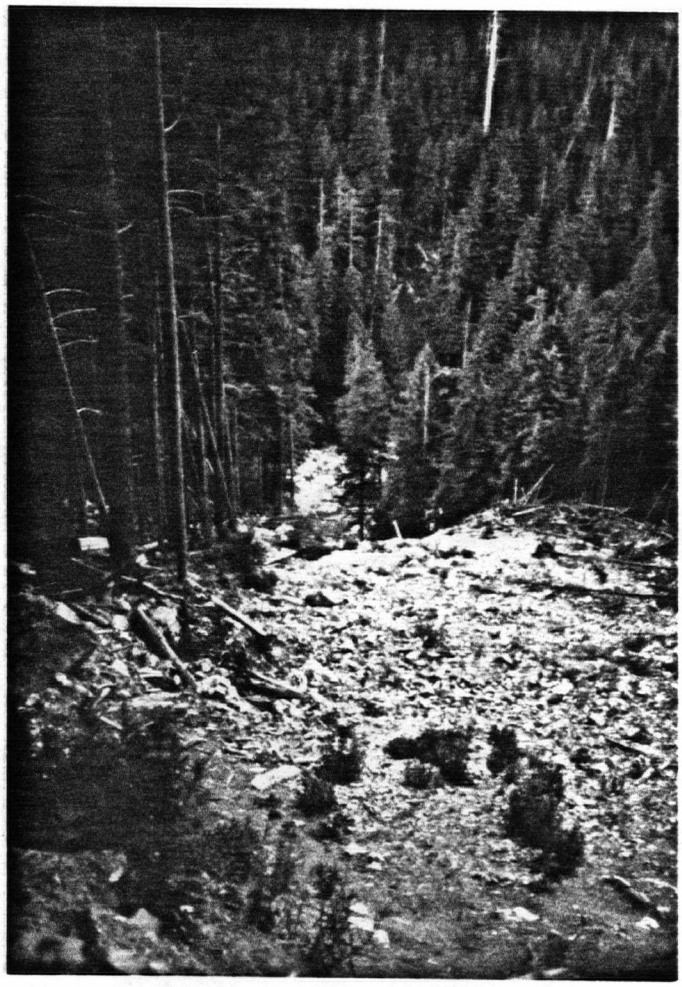

of landslides on aerial photographs have been established (Dishaw, 1967; Poole, 1969; Rib and Liang, 1978). Rice and Foggin (1971) used large scale (1:5000) panchromatic aerial photographs to estimate area affected by soil slippage in the San Dimas Experimental Forest, California. O'Loughlin (1973) used 1:30000 and 1:15000 panchromatic aerial photographs to identify landslides. He reported small scale colour photographs to be of some value in this process, but found colour-infrared photography to be of superior value because of its advantages in detecting age and species differences in stands and the strong bare soil/vegetation contrast provided. Rice et al. (1969), Bailey (1972), and Howes (1987) used a combination of airphoto analysis and ground truth in mapping landslide inventory for stability mapping projects.

Although conventional aerial photography has been used extensively in this field, other remote sensing systems, including Landsat, have been investigated. Gagnon (1975) studied the applicability of various systems in unstable clay formations. He reported that Landsat MSS bands 6 and 7 were useful for study of contrasts in soil water content on a regional level and that thermal infrared scanner imagery was useful for detecting surface water conditions when used in conjunction with infrared black and white photography. This type of imagery was also used to guide fieldwork in an unstable clay area by identifying seepage zones in the area (Tanguay and Chagnon, 1972). Johnson et al. (1977) success-

fully used 1:30000 colour-infrared airphotos to study vegetation anomalies caused by soil moisture changes accompanying movement in incipient slide masses. According to Alfoldi (1974), who worked in similar clay terrain, satellite imagery is useful for its regional perspective, multi-band interpretive capability, and its repetitive coverage upon which detailed investigation may be based. Gimbarzevsky (1983) reported that approximately 40% of landslides in the Queen Charlotte Islands mapped from small scale aerial photographs were visually discernible on MSS band 5, 6 and 7 colour composites. An aircraft mounted radiometer, using Landsat MSS bands, proved useful in a digital classification of slope condition (erosion, deposition, etc.) in an arid region (Pickup and Nelson, 1984). In that study, plots of band ratios for each pixel location provided a classification space for the parameters of interest.

1.3 Object extraction

Object extraction is one approach to recognising patterns of interest in an image. Pattern recognition is a general term which describes the segmentation of a digital image based on a set of class-defining characteristics (Swain and Davis, 1978). When this segmentation is based only on spectral reflectance characteristics of objects in the scene, it is called a classification (Colwell, 1983). Object extraction describes the segmentation of an image using knowledge about the physical shape of image objects as an additional defining characteristic. Swain and Davis

(1978) considered the subject of classification in depth, while Rosenfeld and Weszka (1976) provided a concise review of object extraction.

In object extraction, a decision model based on knowledge about the image gray level conditions that an object exhibits is used to identify object candidates as in a classification. Shape information is generally integrated into the process in region growing, tracking, or template matching systems (Rosenfeld and Weszka, 1976). The result is a segmentation which outlines the object's location in the image. Scenes containing objects with well-defined gray level and shape characteristics set against a predictable background provide suitable input to rigid decision models. However, flexibility is called for in remotely-sensed scenes where gray levels may vary widely from expected values as a result of shadows and atmospheric effects. Furthermore, complex object backgrounds can mimic simplistic object definitions.

1.3.1 Literature review: linear object extraction

Techniques have been developed to recognise a wide range of features in various types of images. Workers in various fields such as medicine and high energy physics report the use of object extraction in their work with imagery. However, this review is limited to work in the recognition of linear objects in aerial and satellite imagery, since this applies to the appearance of Coast Mountain land-

slides in image radiance and shape. A good review of these works is given in Majka (1982).

Majka (1982) described a technique which utilises the primal sketch theory of image understanding (Marr and Hildreth, 1980). Road edges in digitised aerial photographs were defined by the location of the zero crossing "bars" of the Laplacian of the image, and these bars were then evaluated according to geometric criteria. Fischler et al. (1981) reviewed several image operators in developing an integrated approach for identifying linear objects. They categorised these operators as Type I and Type II operators. A Type I operator often misses the feature it is intended to recognise, but commits very few false identifications (commissions). A Type II operator, alternately, accurately identifies the intended features, but makes significant commission errors as well. Their review of operators, which included thresholding, "edge" detection and template matching, did not uncover one which satisfactorily minimised both types of error. Therefore, a methodology was developed which organised the results of such operations according to expected errors in order to optimise the identification process. Tavakoli and Rosenfeld (1982) used a high level of reasoning to organise edge segments in an aerial scene into building and road objects.

There has been interest in the recognition of objects in satellite images as well. Bajcsy and Tavakoli (1976) used

spectral and shape definition of roads to guide the logical discrimination of roads in a satellite image. A hierarchy of feature operators was established which first finds strips with the appropriate geometry and spectral characteristics, then connects these strips according to geometric criteria, and finally thins the resulting "roads". They report 95% recognition in non-urban and 85% recognition in urban areas, although they do not report the rate at which commission errors are produced. Errors were assumed to be due to poor contrast in urban areas and false identifications in non-urban areas. Spatial patterns in a satellite image based on the topographic modulation image (Elisason et al., 1981) have been used to guide the delineation of rivers (Haralick et al., 1982). A "tophat" operator was proposed by Destival and LeMen (1986) to extract roads of various widths in higher resolution satellite imagery. This is a means of simultaneously thresholding spectral edge and physical width information. It is a precedent for the development of specific, task-oriented edge operators based on the type of imagery and object. Shibata (1984) suggested the compatibility of digital elevation data with digital image data. Other work in this field includes that by Bajcsy and Tavakoli (1973), Nevatia and Babu (1979), and Ballard (1981).

These studies contain several common themes. They espouse the use of convolution and/or template operators to extract contrast edge information in the image. They make use of object definitions based on image characteristics and

real world knowledge about the object. Finally, model effectiveness is often evaluated by comparing results to a mapping of the object's locations in the scene drawn from other sources. This study will follow these types of approaches.

1.3.2 A decision model for extraction of landslides

A description of an object's expected representation in the image is preparatory to the design of a model which can suitably detect occurrences of the object. Figure 1.2 shows the satellite image used in the study. Five attributes were chosen to describe landslides:

1. Widths range from 5 metres to 50 metres.
2. Lengths range from a few metres to over 800 metres.
3. Composition is mainly bare soil and rock or revegetation species which contrast with the surroundings.
4. They generally follow the fall line (line of steepest descent).
5. They do not exist to a significant degree at slopes below a certain minimum (10 to 15 degrees).

The depiction of landslides in an enhancement of the image and the DEM will reflect the listed parameters. The image resolution element (pixel) is approximately 30 metres square, and landslides in the image are expected to involve significant numbers of mixed pixels (mixels), with depicted widths of 1 to 3 pixels. This is consistent with the definition of a low resolution linear object. Lengths of object representations (segments) will have an arbitrary lower limit specified in the model ranging to an upper limit of about 30 pixels. Object composition should produce a gray

Figure 1.2. Landsat TM image of the study site. Band 3 (red) is shown in this rendition. The boundary of the study site is shown in black.

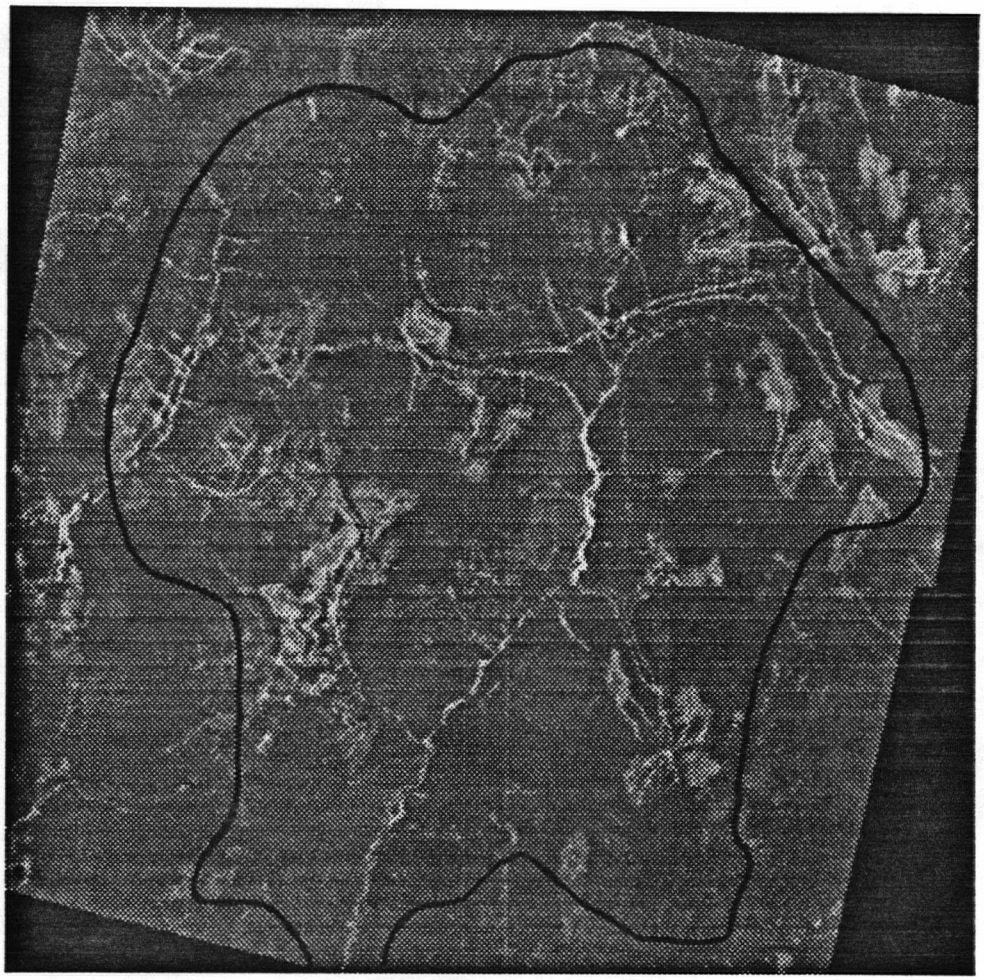

level contrast which is suitable for detection by an edge operator, which in turn will provide object candidates. Slope and orientation attributes will be ascertained from a DEM which is registered to the image. Sufficient information about each candidate will be available in the image and DEM such that a decision can be made about its source (landslide or non-landslide).

The model makes a decision about the source of an image segment based on parameter values associated with the listed attributes. Different values for these parameters will be examined on a trial basis because of their expected variability for the spectrum of landslides in the image. No single trial is expected to be optimum for all landslides. A review of these trials will examine the shortcomings of this approach. The actual parameter values, and the reasoning behind them, are discussed in more detail in Section 3.3.

1.4 Research objectives

This study is an examination of the effectiveness of an object extraction decision model that integrates digital elevation data with a Landsat Thematic Mapper (TM) image. The detection of landslide objects provides the scenario for application of this methodology. The study objectives are:

1. To develop and operate a decision model based on an object definition. A variety of enhanced images will be used to provide candidate segments which fit the definition, and a digital elevation model will be employed to help sort the segments representing landslides from the segments representing other, similar objects in the scene.

2. To evaluate the effectiveness of the decision model by comparing study results to an actual landslide inventory. This evaluation will determine which types of landslides are extracted most reliably. The erroneous identifications (commissions) will also be examined in order to determine how they may be avoided in future applications of this approach.

CHAPTER 2

MATERIALS AND METHODS

2.1 Site description

The study site consists of the Cascade, Norrish, and Deroche creek watersheds as well as an outlying region known as Hatzic woodlot and occupies approximately 150 km^2. The site is primarily underlain by granitic rocks. Present landforms are strongly influenced by the latest (Fraser) glaciation. These effects include oversteepened valley slopes that are overlain with a mantle of glacial till and colluvium whose depth increases downslope, and glacial and glacial-fluvial terraces in the valley bottoms. It is located 65 km east of Vancouver, British Columbia, Canada, and is directly east of Stave Lake and north of the Fraser River (see Figure 2.1). The site is described in more detail by Howes (1987).

2.2 Baseline landslide inventory for the study site

2.2.1 Compilation

Howes (1987) used a statistical approach to a landslide inventory and terrain evaluation scheme on this site of the type introduced by Sondheim and Rollerson (1985). A detailed inventory of the landslide events (Howes, 1985b), as well as a terrain map (Howes, 1985a) was made for that study. The process resulted in a hazard rating map (Howes, 1985c). This inventory consisted of landslides evident on 1:15000 and 1:20000 black and white, vertical photography from 1940,

Figure 2.1. Location map of study site 65 km east of Vancouver (after Howes, 1987).

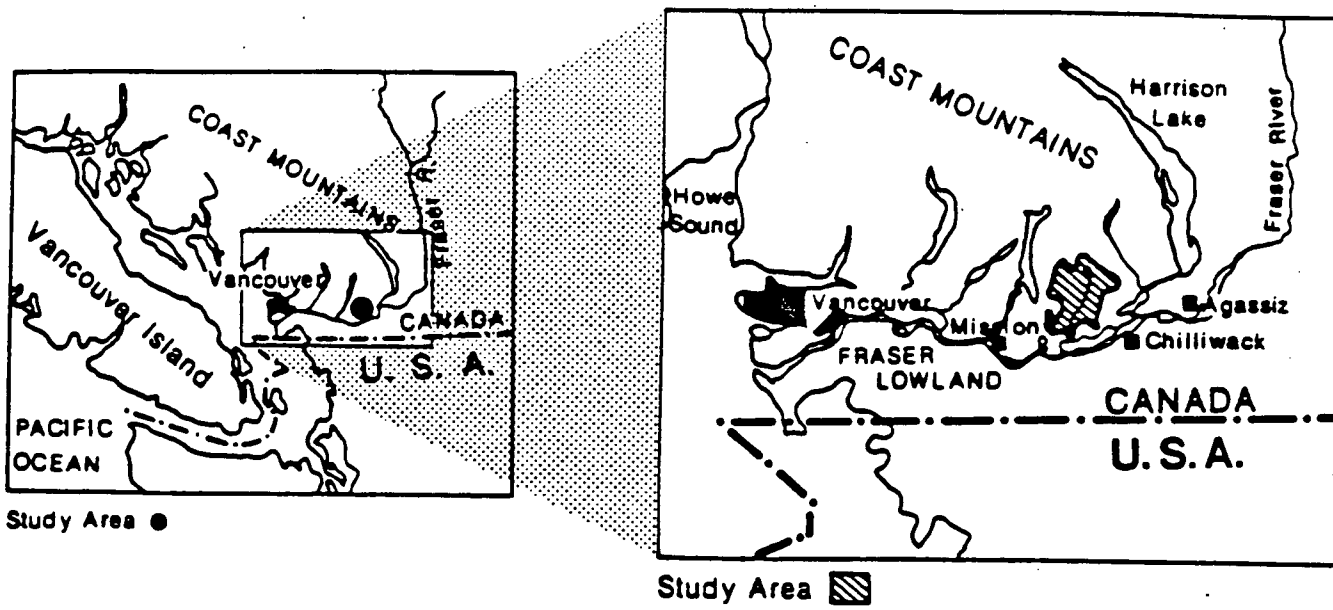

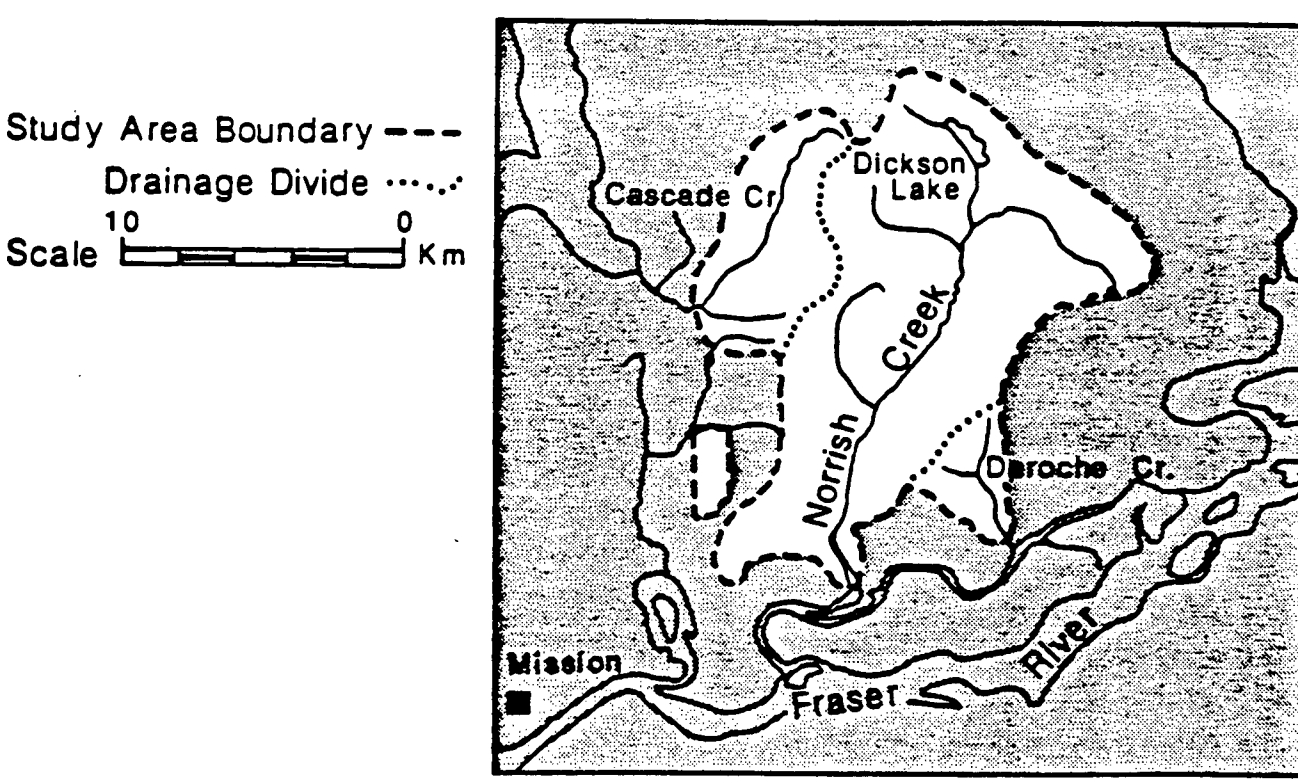

1962, 1968, 1979, and 1981. Besides landslide location, these photos provided information about the approximate date of landslide occurrence and of forest harvest in the area. All landslides in the inventory had a minimum area of 100 m^2 and were identified by established techniques (Howes, 1981). A landslide inventory map was assembled by Howes (1987) from the photos using a 1:20000 base map (photo-enlarged from two 1:50000 NTS topographic sheets) and an epidiascope, a device for photo-to-map transfer (Thomson, 1987). The inventory included detailed information about site characteristics, such as the year of the photography on which the landslide first appeared, for each landslide. Twenty percent of all landslides were field-checked (Howes, 1987).

2.2.2 Data adaptation

One problem with these data is that Howes' minimum size criteria of 100 m^2 was not realistic for the lower resolution TM imagery. A new minimum size criteria was developed based on the Landsat TM resolution of 30 m:

1. Minimum length 150 m.
2. Minimum distance from another landslide 100 m.

The first criterion was based on the assumption that a completely unvegetated slide set at a diagonal to the pixel grid would directly influence pixel values in a minimum string of three pixels length. Other orientations would increase pixel string length. The second criterion was based on an assumption of the scanner's ability to resolve two

distinct, parallel linear objects and is considered a conservative estimate. Landslide groups were developed accordingly.

Given these criteria, Howes' list of 595 landslides for the study area was reduced to 183 single and combination "events" in an event catalogue. The catalogue consisted of 84 landslide groups that were created according to the criteria described above, and which were recorded as single events, as well as 99 unique landslide events. They will be referred to as events throughout the rest of this paper to avoid confusion with the inventory compiled by Howes.

A region of intense landslide activity in the Cascade Creek watershed (CA-48 to CA-64 in Howes' inventory) was eliminated from the study at this point. This region contained a collection of approximately 20 landslides which are predominately less than 100m apart. Any objects detected in this area in the course of the study were not considered in any of the tabulations.

All 183 events in the catalogue were characterised by the following attributes:

1. Photo year of first appearance
2. Photo year of harvest of surrounding site
3. Length
4. Width
5. Aspect
6. Type of event

The first two parameters were obtained from Howes' inventory and the harvest map provided by him. Parameters 3 and 4 were

derived from their appearance on the original inventory map. This was possible since the landslides were depicted on the map to scale. The method is justified by the fact that length and width were required in only 2 classes each. The class boundary between long and short events was 300 m, and the boundary between wide and narrow events was 20 m. These figures divide the data into approximately even subsets, and are consistent with previous efforts to categorise slope movement size (Rollerson, 1987). An average of three separate measures of width (representing the estimated locations of the erosion, secondary deposition, and primary deposition zones) was taken as the width of the event. For a grouped event, the dominant landslide in the group (youngest, largest) was measured. Parameter 5 was also taken off of the inventory map, and parameter 6 was identified for each event by Howes. Appendix C provides the lists of these attributes for all events considered.

Other attributes, such as revegetation state of the landslide and of clearcuts, are of interest, but are much more difficult to quantify objectively. The listed characteristics are analytical, and may be used to infer more subjective properties of the events.

The location of each event was transferred from the 1:20000 map to a set of x and y coordinates using the Terrasoft geographic information system (Digital Resource Systems, Ltd, Nanaimo, BC) installed at the Faculty of

Forestry. This listing was exported to the VAX 11/780 at the UBC Laboratory for Computational Vision (LCV), Department of Computer Science, and read into a plot file format compatible with the software operating the Raster Technologies One (RasterTech) image analysis system installed at the LCV. This file was read from the RasterTech as a standard 512 X 512 image file for use in the study reported in Appendix A.

2.3 Satellite imagery

2.3.1 Image description

A Landsat-5 Thematic Mapper, digital, seven band quarter-scene was acquired by the BC Ministry of Environment and Parks in the summer, 1986 for use in studies in this region. The image was obtained on July 29, 1985 (Track 47, Path 26) and was cloud-free for the study site. A 512 X 512 window of this image was obtained from the Ministry and transferred to the LCV for use there. This window contained the entire study site.

2.3.2 Image band selection

Simplicity dictated the selection of one of the seven available spectral bands for production of the edge images. The selection was based on determining which band provided the greatest contrast across the landslide tracks. A series of transects was made across several known landslides with various characteristics in the image. The results from three

of these transects is shown in Figure 2.2.

These transects represent three distinct forest categories of interest through which the landslides pass: post-1968 harvest, pre-1968 harvest, and no harvest. This information was taken from a harvest history map provided by Howes. This map shows the area of new harvest evident on each set of photos (1940, 1962, 1968, 1979, and 1981). Pre-1968 indicates that an event or harvest first appeared on 1968 (or earlier) photos, and post-1968 indicates it first appeared on 1979 (or later) photos. Areas harvested previous to 1968 are assumed to have regenerated sufficiently such that bare soil and slash are masked. Note the similarity in appearance of the pre-1968 harvest and unharvested transects. This similarity supports the assertion of sufficient regeneration in these areas and is used as the basis for grouping these categories together for the analysis presented in Chapter 4.

According to Figure 2.2, TM band 3, corresponding approximately to red light, and band 2, corresponding to green light, resulted in the highest contrast step across the linear objects in the unenhanced image. Stronger striping, shadows, and haze in band 2 were disadvantages to its candidacy. Band 3 was therefore selected as the source for all edge images.

Figure 2.2. Results from three transects recorded across known landslide tracks. Curves indicate pixel values at each transect location by band.

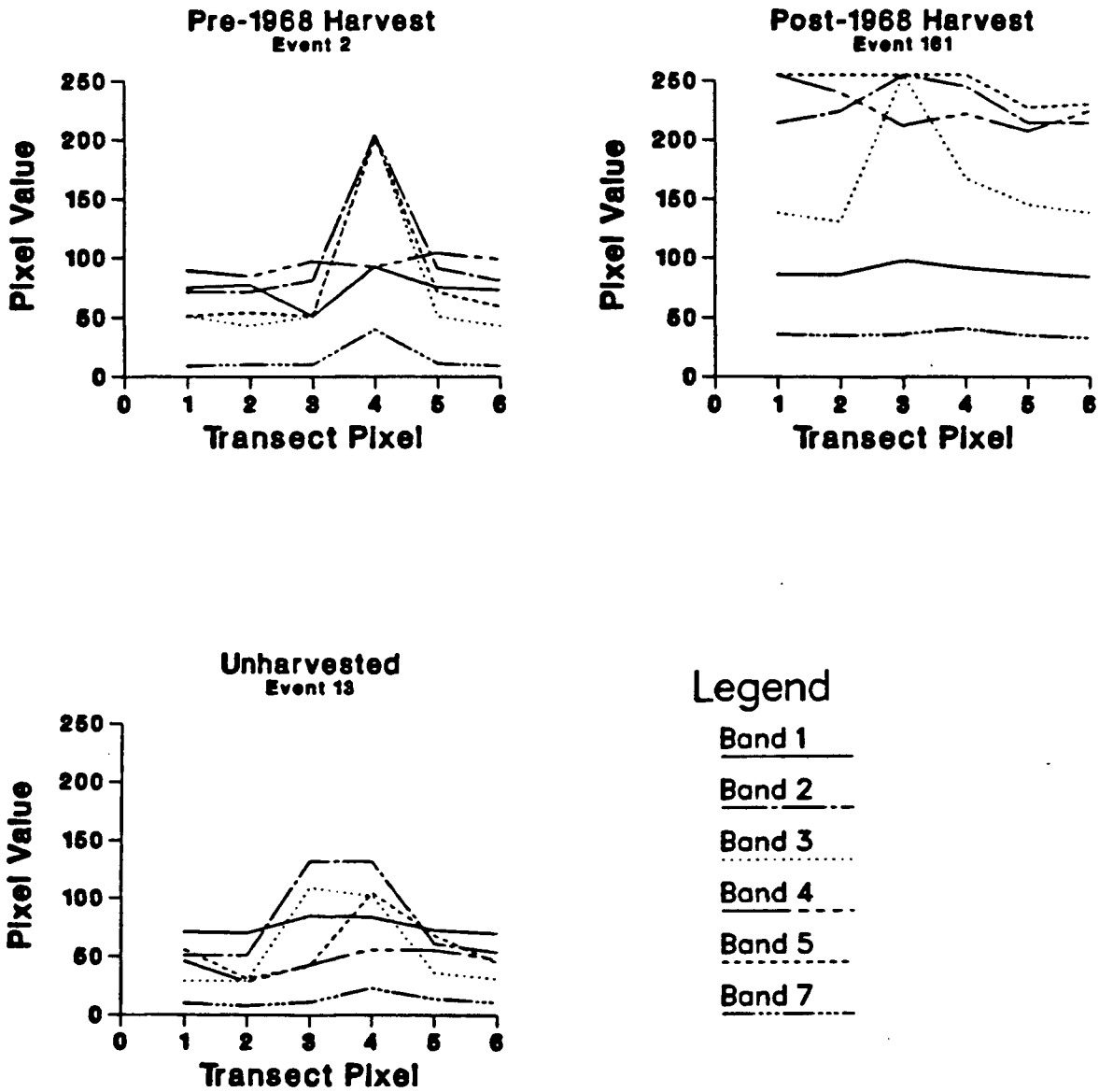

Note: 'Pre-1968 harvest' indicates that the area around the landslide was first noted as harvested on the 1968 (or earlier) photos. Post-1968 indicates that harvest was first noted on the 1979 (or later) photos.

2.3.3 Edge detection

An "edge" is the boundary between two regions of different, constant gray level (Davis, 1975). Therefore, an edge operation is a digital filtering process which, when performed on the image, emphasizes a specific category of contrast edges (Swain and Davis, 1978). By definition, these operations produce new, enhanced images. Since this study is directed to detection and extraction of low resolution linear objects, the edge operations that are investigated produce images where these features are emphasised. These images may then be used for the process of object extraction. They are referred to as enhanced images (or simply edge images) in this paper.

Three diverse approaches were used to provide object candidates for the methodology. In general, these are differential operator, template matching, and threshold/template matching.

2.3.3.1 Differential operator

A differential operator is a point operation which provides a score based on a mathematical assessment of a specific local contrast condition. The condition is recognised as an abrupt change in gray level in a certain direction from a point. The most useful of these, where scene knowledge is limited, is an isotropic operator. The Laplacian is an example of such an operator (Rosenfeld and Weszka, 1976). A practical study of the results of a 3X3 Laplacian operation

showed that this also performed well in finding and emphasizing high brightness, low resolution linear objects in an image. An example of this phenomenon is depicted in Figure 2.3. Consequently, an image was produced using this Laplacian filter on the raw image (Figure 2.4).

It should be noted that where the Laplacian has been mentioned elsewhere (Marr and Hildreth, 1980; Majka, 1982), a Gaussian smoothing has invariably been specified. The purpose of this smoothing is to reduce the effect of image noise and to make the image specific for an intended class of edges. The single pixel noise encountered in Landsat imagery is interpreted as a contrast edge by a 3X3 Laplacian filter. Since the linear objects in this study are generally depicted on the image as 3 pixels wide or less, it was determined that the Gaussian smoothing would produce a mapping that was quite confusing. In effect, the features sought in this study closely resemble the noise that the Laplacian is subject to, and efforts to suppress this noise are counter-productive. The purpose of the study is, therefore, to examine the effectiveness of the methodology in sorting the objects from the noise in such an image.

Another differential operator, known as the Sobel gradient, was considered for use in this study. Like the Laplacian, it is an operator which calculates a two-dimensional derivative at each image point (McManis, 1987). Unlike the Laplacian, however, it is a maximum at the edge of a low

Figure 2.3. A demonstration of the Laplacian operator used in the study. Examples of a simple contrast edge and a low resolution linear are shown.

a) Abrupt, gray scale edge.

```
10 100 100
10 100 100          Laplacian value = 91.
10 100 100
```

b) High brightness, low resolution linear object.

```
10 100 10
10 100 10           Laplacian value = 262.
10 100 10
```

Laplacian kernel:

```
-0.7 -0.5 -0.7
-0.5  4.8 -0.5
-0.7 -0.5 -0.7
```

resolution linear object, not at the centre. Therefore, it would produce a double bar at a low resolution linear object. This ideal was not realized, however, in the complex Landsat image and attempts to translate Sobel image linear representations into single bar tokens were frustrated by the variability in image values. For that reason, this operator was not considered further.

2.3.3.2 Template Matching

If an object has a known geometry, it is possible to construct a template that, when scanned over the image, will

Figure 2.4. The Laplacian edge image used in the study. The 3X3 kernel shown in is in Figure 2.4 was used to calculate this image.

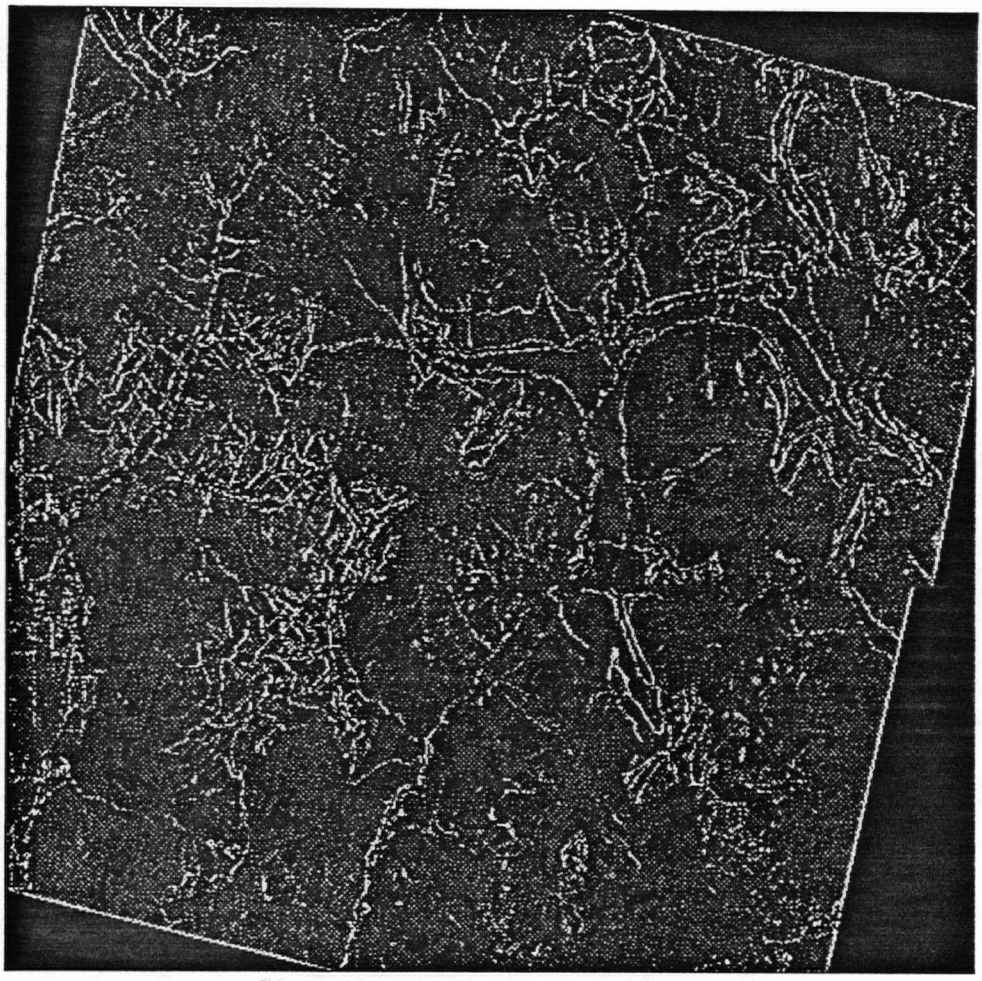

assign a suitable score to occurrences of a gray scale/shape combination in the image which fits the description. If the direction of the object is not specified, a series of orientations to the template may be presented. One example is the Duda Road Operator described by Fischler et al. (1981). This operator looks for segments of three pixel's length in the two cardinal directions and the diagonals. It is described as a Type I operator in their terminology because it is prone to errors of omission. This may be partly attributed to its inability to recognise segments not within these directional constraints (those three pixel segments which would be represented as a "jog", instead of a linear alignment). Two out of the four masks used in this approach are shown in Figure 2.5. A review of the calculations associated with this filter is omitted here.

Since information ancillary to the image data (i.e. topography) is available in this study, the directional limits which are evident in the above example could be relaxed in an effort to reduce potential omissions. A landslide template reflecting this concept is shown in Figure 2.6. It is conceptually different from the road operator since calculations for all directions are made during a single pass of the filter. Note that the directional constraints are relaxed in comparison to the road operator since the four, two pixel segments (which the operator examines at each point) represent all possibilities (see Appendix D for further discussion of this topic). The con-

Figure 2.5. The Duda Road Operator as presented by Fischler et al. (1981). This is an example of a template matching scheme. Note that a total of four operations is required to produce the final "edge" image. The score for the a2 pixel is taken as the maximum of these four trials.

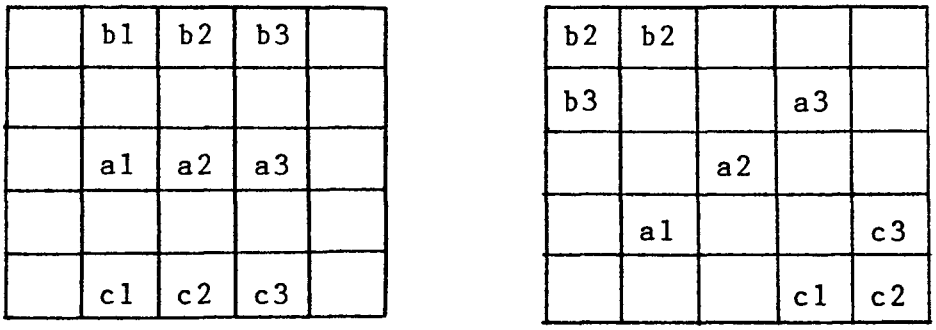

Figure 2.6. The landslide operator developed for the study. Note that all four directions are considered during one pass. Appendix D addresses an oversight in this template.

A	B	C	D	E
F	G	H	I	J
K	L	M	N	O
P	Q	R	S	T
U	V	W	X	Y

SCORE1 = L - (B+V)/2 + M - (W+C)/2

SCORE2 = G - (P+D)/2 + M - (U+E)/2

SCORE3 = H - (F+J)/2 + M - (K+O)/2

SCORE4 = I - (B+T)/2 + M - (A+Y)/2

FINAL SCORE = MAXIMUM OF 4 SCORES.

trast measurement is taken at a one pixel distance, as in the road operator, so that edge, or mixel, effects near the boundary of the desired linear are reduced. The highest score from the four directions is taken as the output value at the centre. The resulting image used in this study is shown in Figure 2.7.

2.3.3.3 Threshold/template matching

A simple image intensity threshold may be sufficient to delineate a feature when that feature is primarily distinct for its presence at a particular intensity range to the general exclusion of other image features. This method has been employed for the extraction of low resolution linear objects (Fischler et al., 1981), and is quite flexible in its application. A histogram of image intensity values is useful in determining the gray level at which to threshold, especially in an image dominated by two objects (Weszka, 1978). Although a Landsat scene is much more complex, a histogram may still guide a thresholding procedure.

If we assume that the image histogram mode (see Figure 2.8) represents the dominant feature in the scene (in this case old-growth forest), then pixel values in landslide tracks of the type under consideration should lie to the right of that value, since they are generally brighter in this band due to soil exposure. Edge effects from surrounding vegetation certainly play a role in the signature of these pixels, and the landslides occur in both harvested and

Figure 2.7. The landslide template image used in the study. The raw satellite image was used in producing this image using the landslide template.

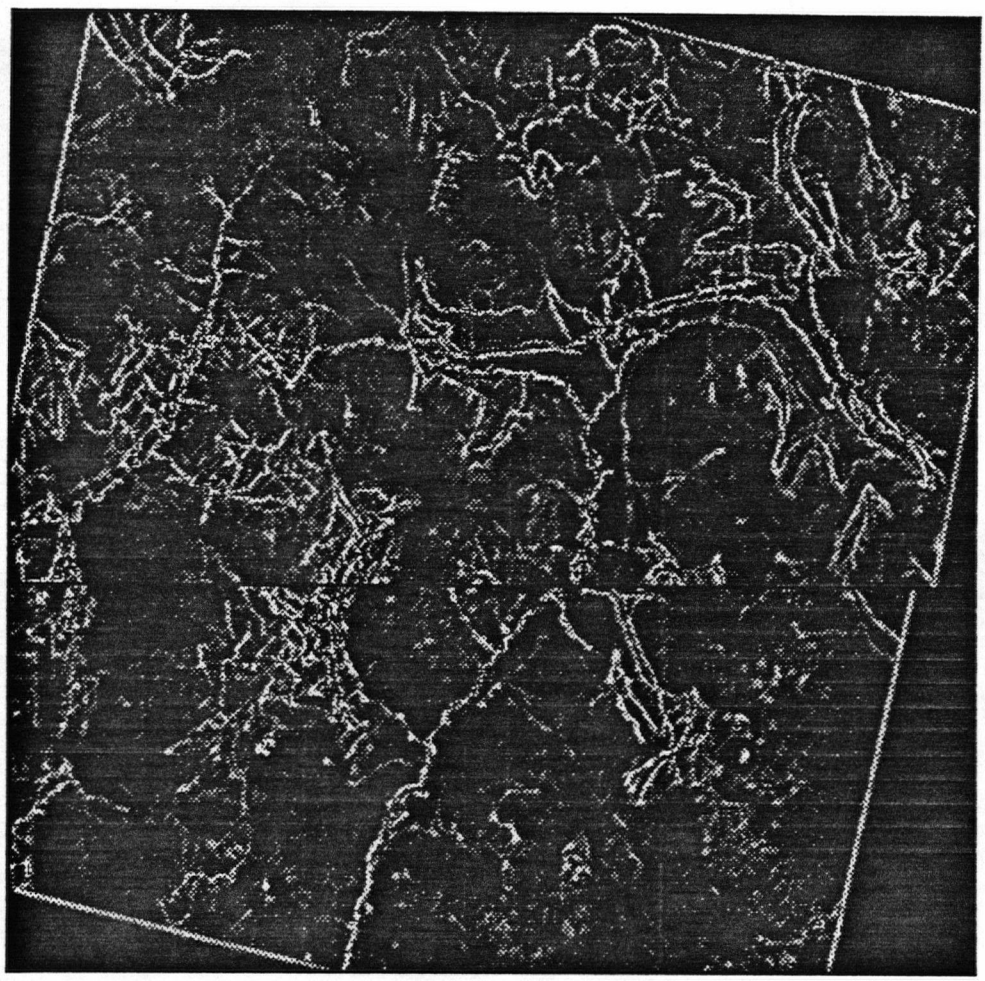

Figure 2.8. Histogram of image band 3 of the study site. Arrows indicate threshold values used to produce the threshold/template matching image.

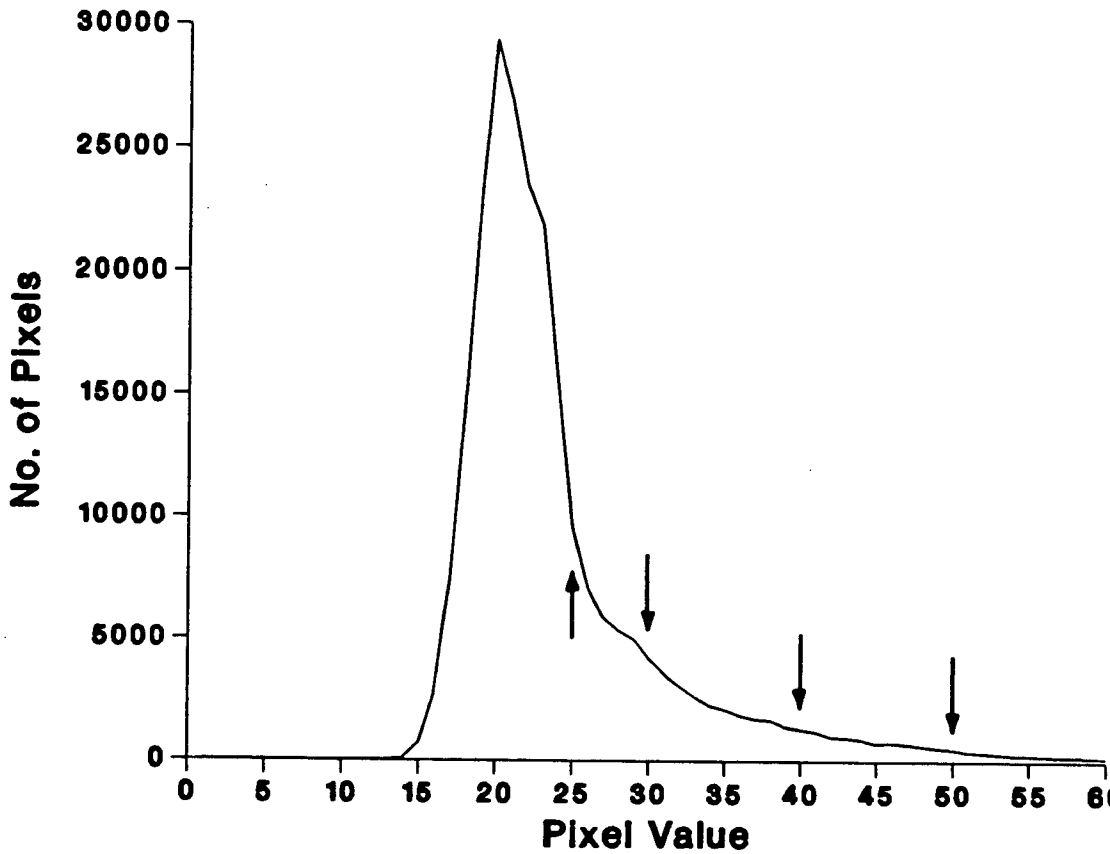

unharvested areas in various states of regeneration, producing further effects. Therefore, four thresholds (of raw image pixel values) were specified in order to emphasize landslides in various conditions: 25, 30, 40, 50 (mode = 20). The landslide template (described above) was run on each thresholded image in order to isolate the linear objects in the thresholded images from objects of other shapes. The resulting images were summed to produce a final, binary image for use in the methodology (see Figure 2.9a-e).

2.4 Digital topography

Topographic contours from the 1:20000 base map were digitised into two files (due to software limitations), and were subsequently translated to a regular 40m grid network (due to software limitations) using the Terrasoft system. This grid was exported to LCV, where the grid was resampled to 30m to match the approximate pixel dimension of the TM scene, and thus could be manipulated as an image file. Display of the site from a "synthetic" view, as shown in Figure 2.10, is an example of one such manipulation. This image was produced using the "synthetic" program at the LCV which assumes a Lambertian surface and in which the sun angle and location may be specified.

The synthetic view, with the sun at 45^{o} above the horizon and at the northwest, revealed three problems with the gridded topography: a "stepped" effect on the hill-

Figure 2.9a-d. The northwest quarter of the scene (image band 3) thresholded at 4 pixel values. a) 25 b) 30 c) 40 d) 50. Note how different linear objects appear at different thresholds.

a.

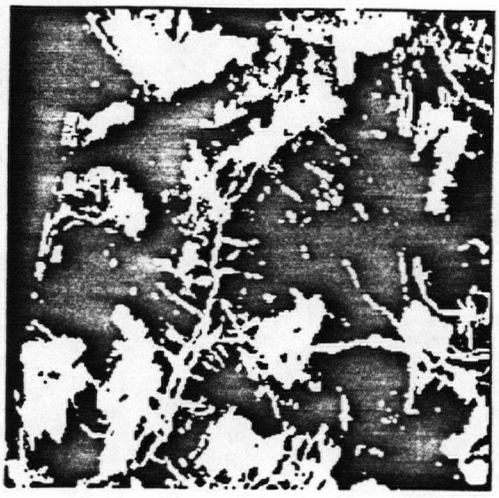

b.

c.

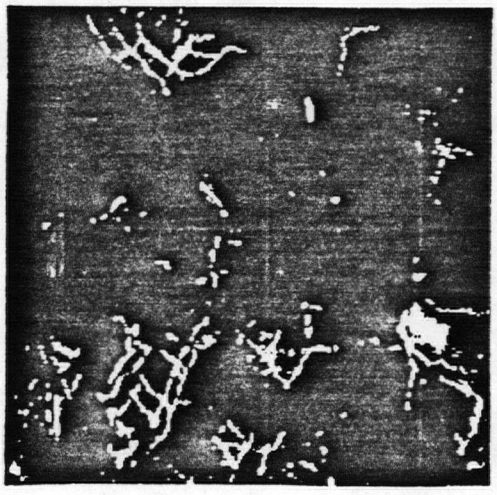

d.

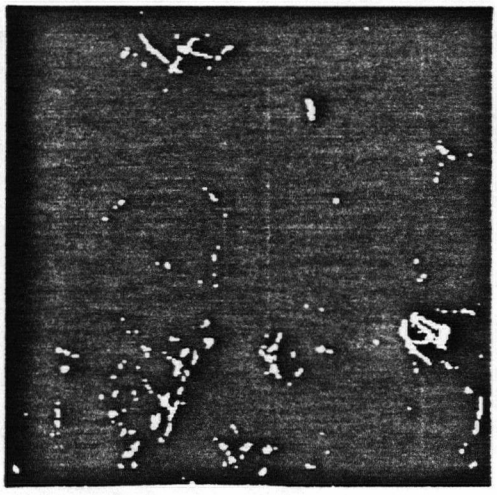

Figure 2.9e). The threshold/template matching image used in the study. This is a composite of the 4 threshold images (each reduced to linear objects using the template described in Section 2.3.3.2).

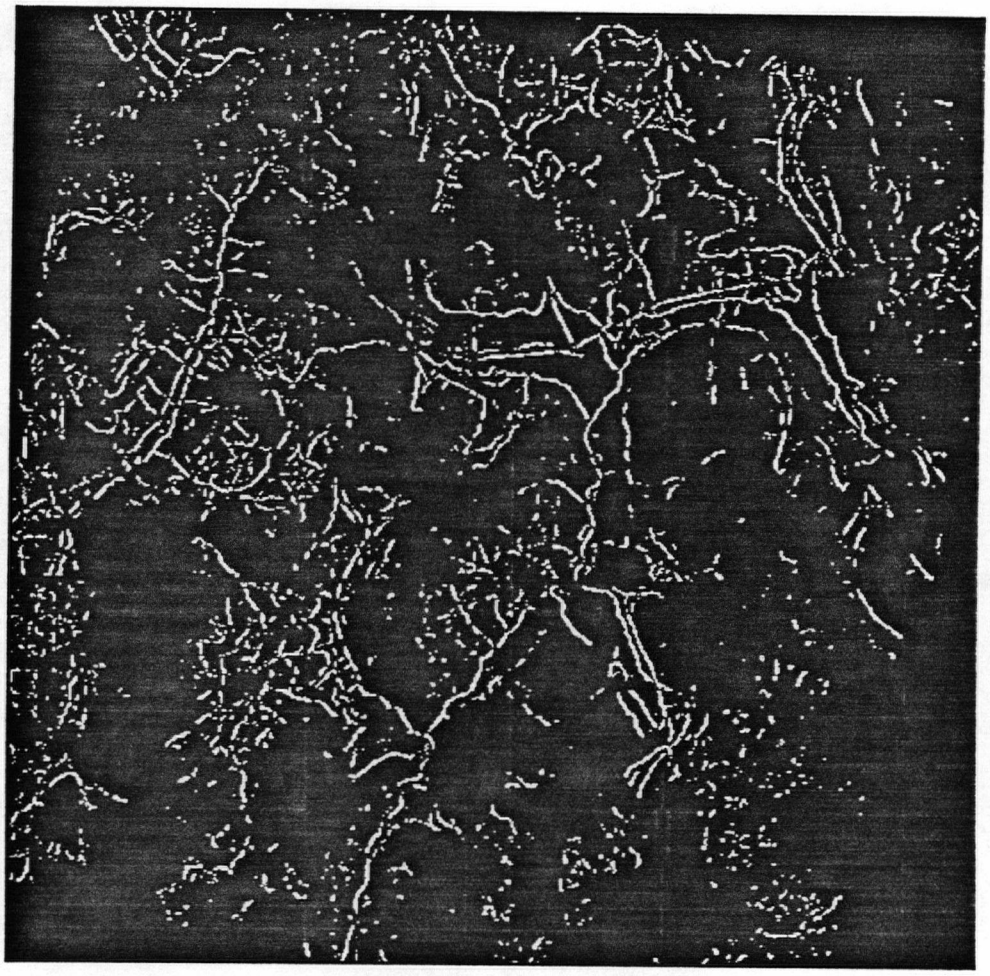

Figure 2.10. Synthetic view of the digital elevation model of the study site. A Lambertian surface is assumed and the sun is at 45° above the horizon in the northwest. Note the "stairsteps" along the cardinal axes which would cause significant errors given a simple, point slope calculation.

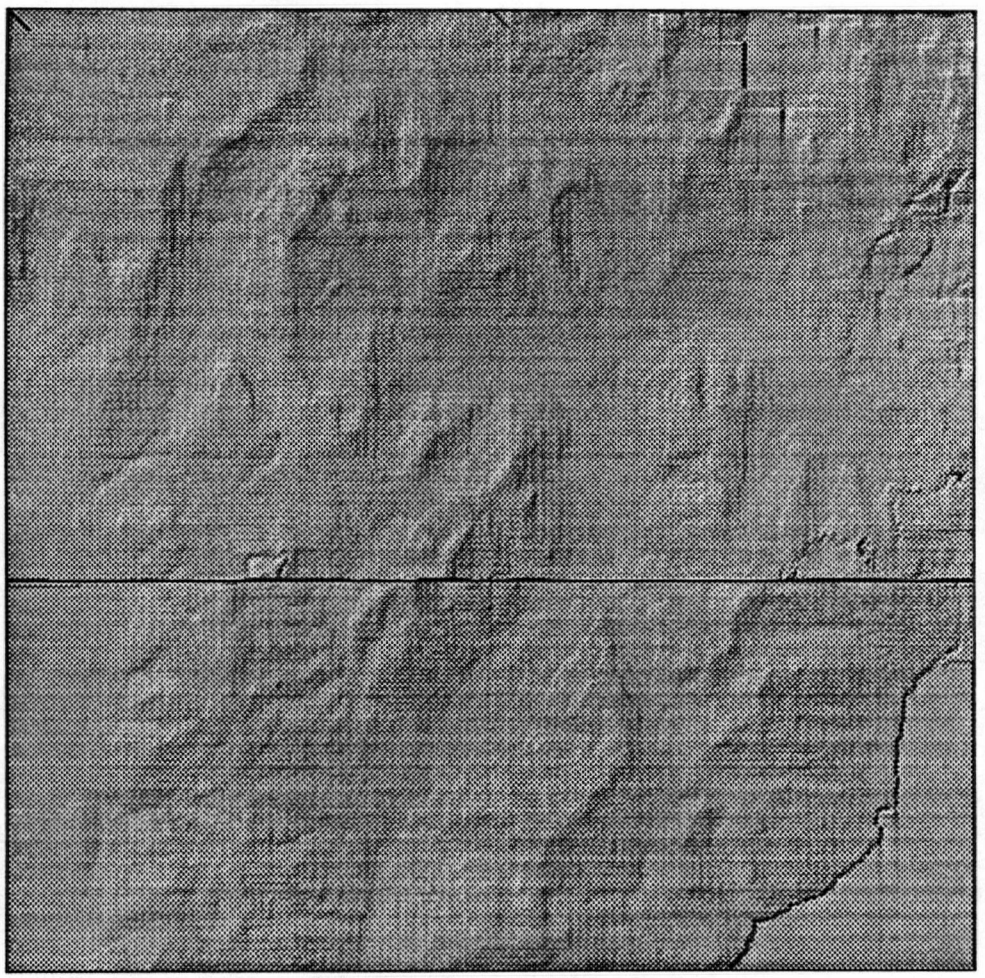

slopes, a "T" appearance at the summits (not evident in Figure 2.10), and an abrupt edge at the mating of the two sections. The improper mate line is an artifact of a registration problem at the digitiser, and represents some loss of data and geometric integrity. Since minor geometric problems can be accommodated in the image to map registration process and the loss of data is restricted to a small percentage of the study area, this problem did not necessitate re-entry of the data. The first two may be explained as artifacts of the gridding routine that was used. A weighted average is used in the routine for interpolating grid intersection values from grid/contour intersection values (Digital Resource Systems Ltd, 1987). This is not a rigorous evaluation of the physical relationship of these points. The summit "T" is caused by the consideration of contour intersections along grid lines only when grid point values are being interpolated and the improper weighting of these values in the interpolations. The "T" ramps follow these grid lines. The "stepped" hillslope is of greater consequence to this study. It is due to the improper weighting of cross-slope contour intersections in the interpolation process.

Since no other gridding algorithm was available at the time of this study, a method was sought that would mitigate the adverse effect that the poorly gridded data would have on calculated slopes. Mode filters of various sizes produced unrealistic artifacts at ridge and valley locations and were

deemed unsuitable. An "intelligent" averaging filter was devised for producing a workable slope file.

The slope algorithm which was used is shown in Figure 2.11. It is based on the observation that the steps in the synthetic view were between 1 and 2 pixels long and always set across the slope along the cardinal axes. The difference between A and B and between C and D was obtained, and the ratio of these differences was taken as the tangent of an angle from which a fall line azimuth (AZIMUTH) was derived. The slope gradient across each pixel was estimated by weighting the drop across four pixels in each cardinal direction according to the AZIMUTH vector.

Two coded raster files were created from this exercise. The first contained an integer value at each pixel location which represented the estimated drop in metres across that pixel, and the second contained integer values from one to nine which indicated the pixel through which the AZIMUTH vector passed (i.e. the pixel which was directly downhill of the one under consideration). The code format for this second file is shown in Figure 2.12. These two files were the source of program arrays DROP and DIRECTION respectively (as described in Section 3.2).

Figure 2.11. The slope adjustment operator used to estimate point slope values from the digital elevation data.

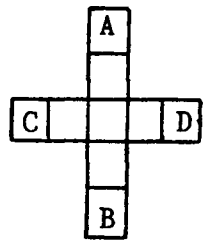

FALL LINE CALCULATION

$$ANGLE = ARCTAN(A-B)/(C-D)$$

(Where: $C-D \neq 0$)

If $C-D > 0$

$$AZIMUTH = 90^{o} + ANGLE$$

If $C-D < 0$

$$AZIMUTH = 270^{o} + ANGLE$$

SLOPE CALCULATION

$$DROP = (|A-B|*(|ANGLE|/90^{o}) + |C-D|*(1 - (|ANGLE|/90^{o})))/4$$

DEFINITIONS:

ANGLE is an intermediate value for fall line calculation

AZIMUTH is the azimuth value of the fall line vector.

DROP is the estimated drop across the centre pixel in metres.

Figure 2.12. Code format for the fall line vector file. An integer value from 1 to 9 at pixel X indicates the direction of the fall line according to this code.

1 2 3

4 X 6

7 8 9

CHAPTER 3

IMPLEMENTATION

The study was carried out in two parts. The first part demonstrates the usefulness of an edge enhanced image for detecting landslides using a linear segment object definition without elevation information. Since it was only intended to examine the validity of using such images in an automated methodology, and does not constitute a viable method of meaningful image segmentation by itself, it is presented as an appendix (Appendix A) to this paper.

The automated methodology presented here sorts the segments representing the landslides from the segments representing other objects in three edge images by integrating a DEM into an automated technique. Results show the type of landslides which are sorted best, while indicating the shortcomings of this method in terms of data quality and model simplicity.

3.1 Introduction

The Landsat image was registered to the DEM in three sections: northwest section, northeast section, and south section. Control points for this registration included valley road intersections, river crossings and points, and other features represented on the map. The three edge operations as described in Chapter 2 were performed on this image.

Four criteria for landslide detection were specified for each edge image:

1. Pixel value above a specified value.
2. Minimum segment length in pixels.
3. Minimum slope at each pixel.
4. Candidate segments oriented along the fall line.

These criteria were employed in an image analysis program written in the C programming language at the LCV.

3.2 Image evaluation program

Three files were necessary for program operation: slope direction (DIRECTION), slope magnitude (DROP) and the edge image under consideration (IMAGE). Three user specifications were also necessary to guide each trial: image threshold value, minimum slope, and minimum segment length. Once input files were read into program arrays (DIRECTION, DROP, and IMAGE) and the edge image was thresholded according to specification, program operation commenced as two consecutive exercises: segment identification and segment length appraisal. The pseudocode fragments in Figures 3.1 and 3.2 highlight these two processes respectively. Figure 3.3 provides definitions for the terms used in Figures 3.1 and 3.2.

In segment identification, each candidate pixel (an edge image pixel whose value is greater than the specified threshold) is evaluated according to its neighbours' values. If the neighbour which is downhill from it is also a candidate, then the pixel location is assigned a value of 4 in

Figure 3.1. Pseudocode for segment identification.

```
initialize array designators r and c;

  begin loop, increment c by 1;
  if (IMAGE[r][c] is equal to 1)
    solve for r1 and c1 using DIRECTION[r][c];

    if (IMAGE[r1][c1] is equal to 1 and
    DROP[r][c] is greater than minslope)
      solve for upslope as an inverse of DIRECTION[r][c];
      solve for r2 and c2 using upslope;

      if (IMAGE[r2][c2] is equal to 1 and
      DROP[r2][c2] is greater than minslope)
        set INTER[r][c] equal to 3;
      otherwise, set INTER[r][c] equal to 4;

    otherwise, set INTER[r][c] equal to 2;

  otherwise, set INTER[r][c] equal to 0;

  if (c is less than the width of the image)
    return to beginning of loop;
  otherwise, increment r by 1;
  if (r is greater than the length of the image)
    jump out of loop;
  otherwise, return to beginning of loop;

  end.
```

See definitions in Figure 3.3.

Figure 3.2. Pseudocode for segment length appraisal.

```
initialize array designators r and c;

  begin loop, initialize counter1 and counter2;
  increment c by 1;
  if (INTER[r][c] is equal to 4)
    set s equal to r and set t equal to c;
    begin loop, increment counter1 by 1;
    solve for r1 and c1 using DIRECTION[s][t];

    if (INTER[r1][c1] is equal to 3)
      set s equal to r1 and t equal to c1;
      return to beginning of loop;
    otherwise, jump out of loop;

    set s equal to r and t equal to c;
    begin loop, increment counter2 by 1;

    if (counter1 is greater than or equal to minlength)
      set (OPIX[s][t] equal to 5);
    otherwise, set OPIX[s][t] equal to 0;
    solve for r1 and c1 using DIRECTION[s][t];
    set s equal to r1 and t equal to c1;

    if (counter2 is equal to counter1)
      jump out of the loop;
    otherwise, return to beginning of loop;

  otherwise, set OPIX[r][c] equal to 0;

  if (c is less than the width of the image)
    return to beginning of loop;
  otherwise, increment r by 1;
  if (r is greater than the length of the image)
    jump out of loop;
  otherwise, return to beginning of loop;

  end.
```

See definitions in Figure 3.3.

Figure 3.3. Definitions for variables used in Figures 3.1 and 3.2.

IMAGE is an array containing edge image information:
  1 indicates edge image pixel greater than specified threshold.
  0 indicates edge image pixel less than specified threshold.

DIRECTION is an array with member values 1 to 9. The value indicates the pixel which is directly downhill of the present one.

DROP is an array indicating metres of drop across the pixel.

INTER is an array for storing segment identification results.
  4 indicates segment beginning (top of landslide candidate).
  3 indicates segment middle.
  2 indicates segment end or pixel that has failed the trial criteria.
  0 indicates no segment.

r & c designate array member under consideration.

r1 & c1 designate array member downhill from the present one.

r2 & c2 designate array member uphill from the present one.

a & b are used to store array designator values.

minslope is the designated minimum landslide slope.

upslope is used to store the inverse of slope[r][c].

OPIX is an array for storing results.
  5 indicates landslide identification success.
  0 indicates landslide identification failure.

s & t are used to store array designator values.

minlength is the designated minimum segment length.

counter1 is used to count segment members in initial evaluation.

counter2 is used to count segment members during opix write.

the intermediate result array (INTER) which indicates a segment beginning. If the neighbour directly uphill is also a candidate, then the pixel location is assigned a value of 3 in INTER which indicates the middle of a segment. Candidate pixels which fail the first test are assigned a value of 2. Consequently, the lowest elevation member of a processed segment is implied by the appearance of a 2 downhill from a 3 in INTER.

INTER serves as the input to the segment length appraisal process. If a 4 is encountered in the array, a 3 is sought at the downhill vector location, and a 3 is subsequently sought downhill from that location, and so on, while a counter tracks the number of pixels in the segment. If the segment is as long or longer than the minimum specified at the start, then each pixel is written as a 5 to the output array (OPIX). Alternately, each location is written as a 0. When completed, OPIX is written as an image file which serves as the visual result of the trial, or a "landslide image."

3.3 Landslide image production and evaluation procedure

In all, 14 trials were run and 14 landslide images produced: 6 each for Laplacian and template edge images, and 2 for the threshold/template matching edge image. These trials are outlined in Table 3.1. Each trial was evaluated for percent successes and percent commission errors before the next one was specified. The study was limited to the

consideration of 2 thresholds of the edge image (where applicable), 4 minimum slope values, and 2 segment length values.

Two threshold values were determined from each edge image histogram, approximating the pixel value at 50% and 25% of the number of pixels at the histogram peak. These histograms and corresponding threshold values are shown in Figures 3.4 and 3.5. The thresholding was not relevant for the threshold/template image, as it was already a binary image. The 2 segment lengths of 4 and 5 were within the range of minimum landslide length under consideration (at least for cardinal orientations). A value of 3 was ruled out as prone to commission error production, as was the connection of 2 pixel segments (as specified in Appendix A). Slope values of 10^{o}, 15^{o}, 20^{o} and 25^{o} could be considered for each operator. This is based on world knowledge of actual landslide occurrence where slopes below a minimum value quickly reduce the driving force behind a landslide (VanDine, 1985).

Images were evaluated by visual verification of each segment in the landslide image. The landslide image was displayed as an overlay on the satellite image, and image features oriented the user to the position of the segments on a set of 1982, 1:40000 black and white vertical airphotos and on the landslide inventory map. If a segment coincided in position and orientation to all or a portion of a catalogued landslide location, it was recorded as a successful identification. The incidence of a commission error was

Table 3.1 Trial layout for landslide image production

Trial	Operator	Image threshold	Minimum slope (degrees)	Segment length (pixels)
A	Laplacian	5	25	4
B	Laplacian	5	20	4
C	Laplacian	5	20	5
D	Laplacian	7	20	5
E	Laplacian	7	15	5
F	Laplacian	7	20	4
G	template	2	20	4
H	template	2	20	5
I	template	2	25	5
J	template	3	15	5
K	template	3	20	5
L	template	3	20	4
M	thr./tem.	-	15	4
N	thr./tem.	-	10	4

Note: Slope in degrees is translated to drop across a 30 m pixel in the model.

Figure 3.4. Histogram of Laplacian image. Arrows indicate threshold values used.

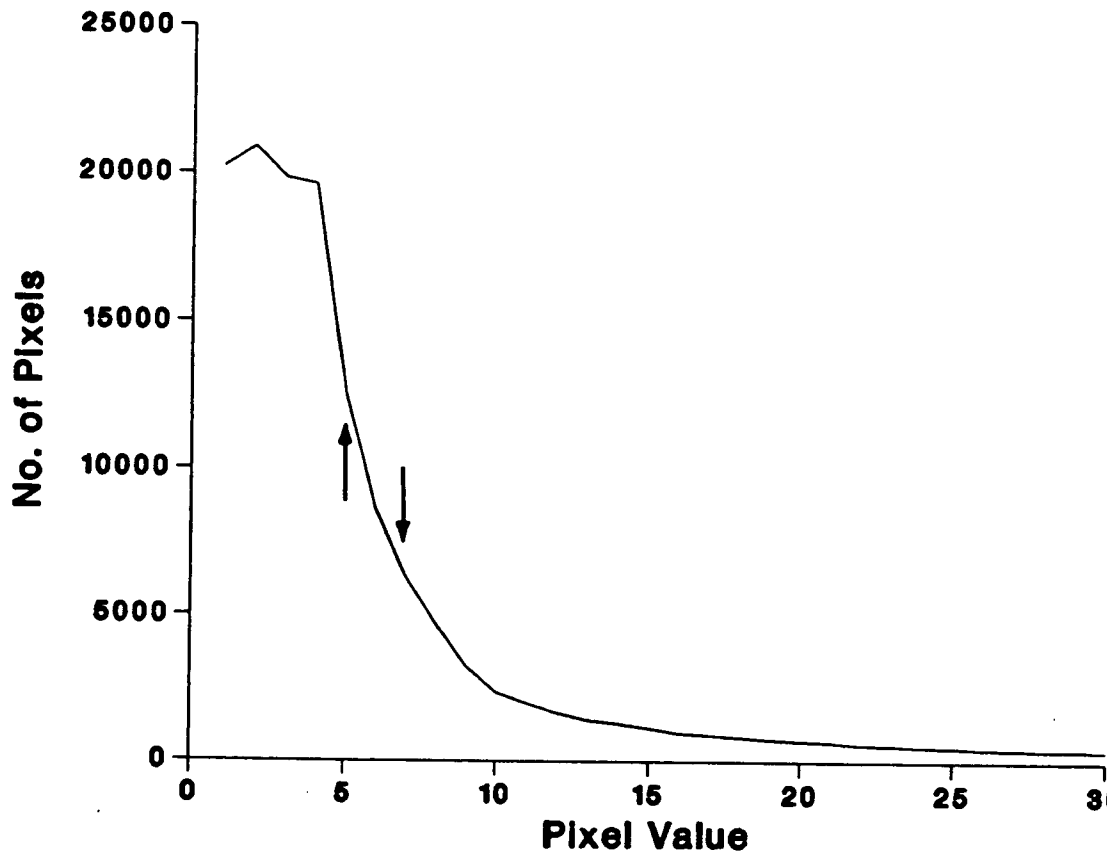

Figure 3.5. Histogram of template matching image. Arrows indicate threshold values used.

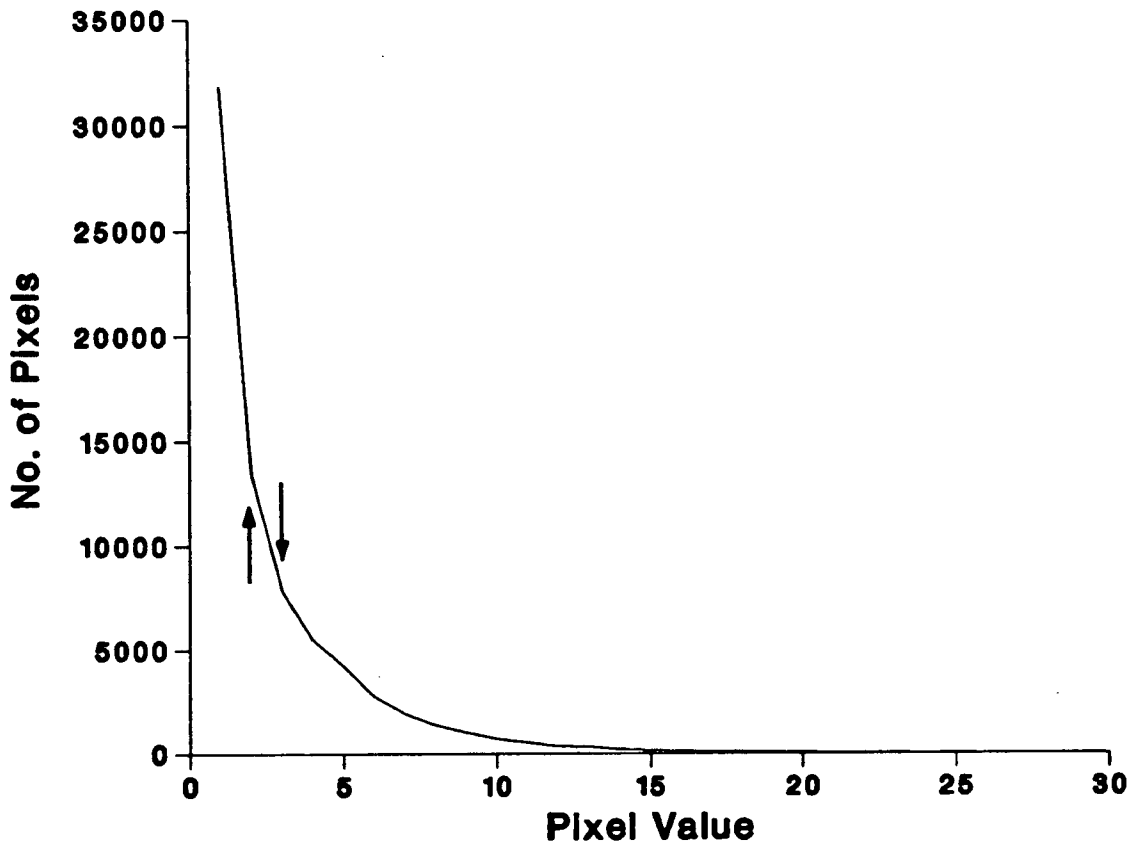

recorded separately. Trials with a commission rate of less than 50% were deemed of interest since they are associated with greater user confidence in an object identification system. If commission errors were less than 50% of the total number of identifications in a trial, then the apparent cause of the error, as identified from airphoto and image evidence, was recorded.

The following rule guided the procedure for choosing the parameters for subsequent trials on each edge image. For each trial, if the commission errors exceeded 50% of the identifications made, then the next trial must not vary a parameter in such a way that an increase in commission errors could be expected. In this way, the process was guided to find the most reliable operations. Two trials, each with commission rates of 49%, were grouped with the trials over 49%.

CHAPTER 4

RESULTS AND DISCUSSION

4.1 Results

Success and commission results for the 14 trials studied are shown in Table 4.1. Trials with less than 50% commission rates were considered in a detailed analysis. Seven trials (D,M,K,N,E,I,J) fulfilled this requirement. Trials I and J, however, at 49%, were not considered for detailed analysis. The remaining 5 trials represent 2 each from the Laplacian and threshold images and 1 from the template image. Three properties of these trials are of interest in the evaluation of the methodology: what are the causes of the commission errors and what are the characteristics of the events that were and were not identified? Answers to these questions will indicate the usefulness of this approach and point out where improvements could be made.

The segments which indicate landslide locations for the 5 selected trials are displayed in black against the satellite scene in Figures 4.1 to 4.5. The location of each segment indicates a correct identification or a commission error. These images were reviewed in detail in order to categorise each segment.

4.1.1 Commission errors

Commission errors were labeled and their probable cause indicated from photo evidence (see Appendix B). Of the 77

Table 4.1. Success and commission results for 14 trials.

Rank by Commission	Rank by Success	Trial	Operator	Success %	Success No.	Commission %	Commission No.
1	14	D	Laplacian	18	33	35	18
2	11	M	thr./temp.	23	42	35	23
3	9	K	template	24	45	37	26
4	8	N	thr./temp.	28	51	41	35
5	7	E	Laplacian	28	51	41	36
6	12	I	template	19	36	49	34
7	3	J	template	36	67	49	65
8	6	F	Laplacian	31	57	50	56
9	10	C	Laplacian	24	45	51	47
10	4	H	template	36	66	53	73
11	5	L	template	34	62	55	76
12	1	G	template	48	89	62	147
13	2	B	Laplacian	37	68	70	158
14	13	A	Laplacian	19	35	70	83

Trial references are in Table 3.1.

Trials above horizontal line were considered in analysis.

Figure 4.1. Trial D (Laplacian operator). Northwest quarter of scene is shown, with identifications shown in black. Compare the number of black segments here with the white segments in Figure 2.5.

Figure 4.2. Trial M (Threshold/template operator). Northwest quarter of scene is shown, with identifications shown in black. Compare black the number of black segments here with the white segments in Figure 2.10e.

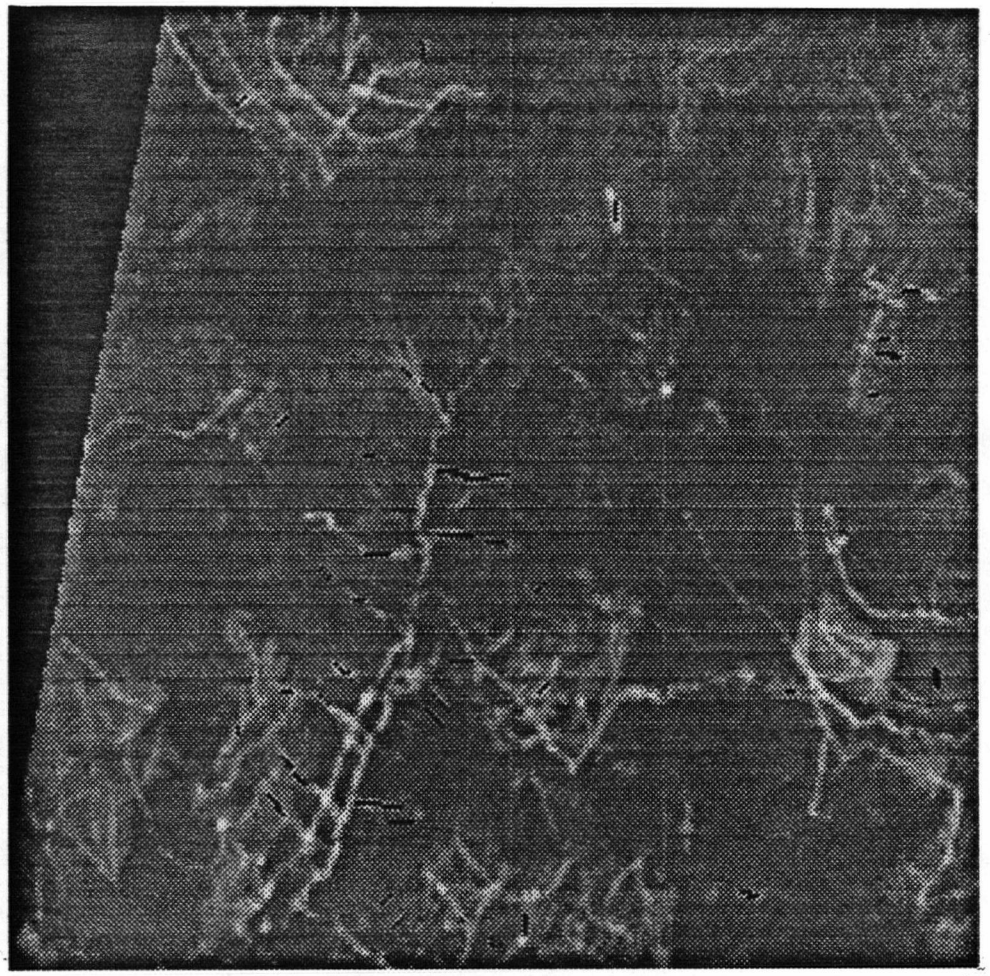

Figure 4.3. Trial K (Template operator). Northwest quarter of scene is shown, with identifications shown in black. Compare the number of black segments here with the white segments in Figure 2.8.

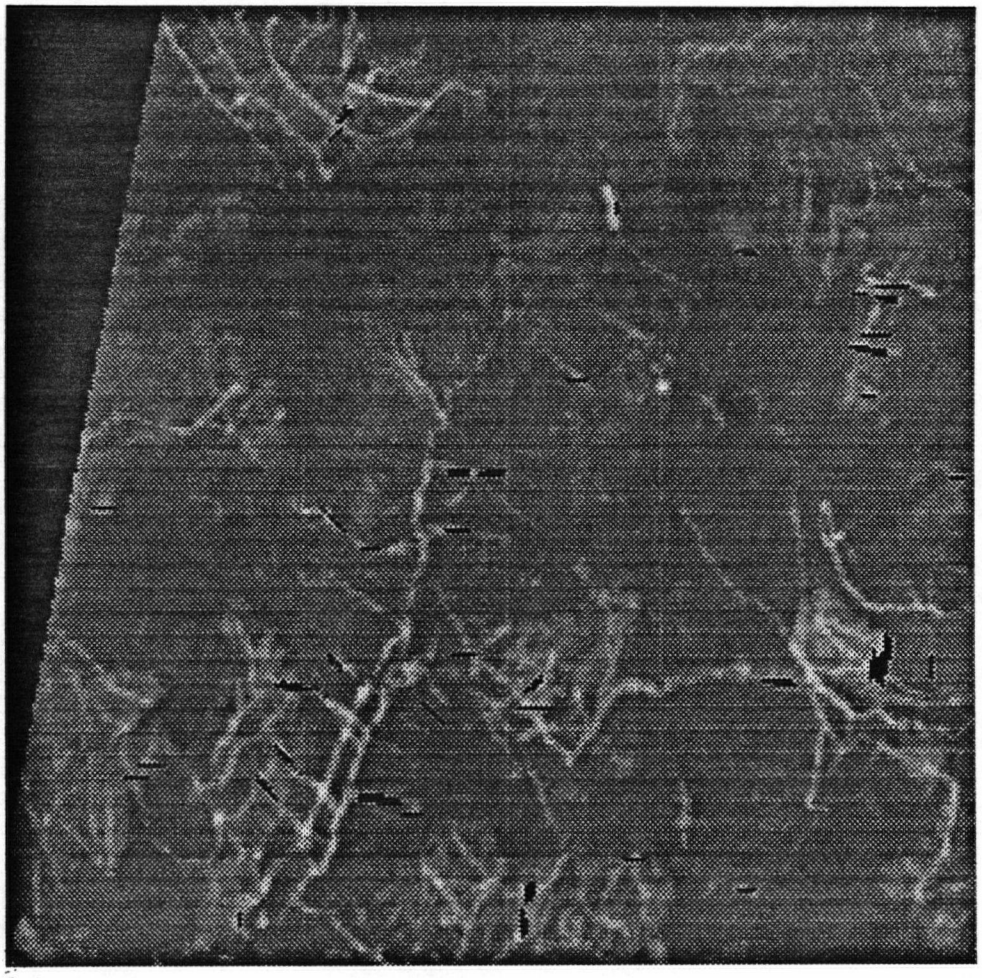

Figure 4.4. Trial N (Threshold/template operator). Northwest quarter of scene is shown, with identifications shown in black. Compare the number of black segments here with the white segments in Figure 2.10e.

Figure 4.5. Trial E (Laplacian operator). Northwest quarter of scene is shown, with identifications shown in black. Compare the number of black segments here with the white segments in Figure 2.5.

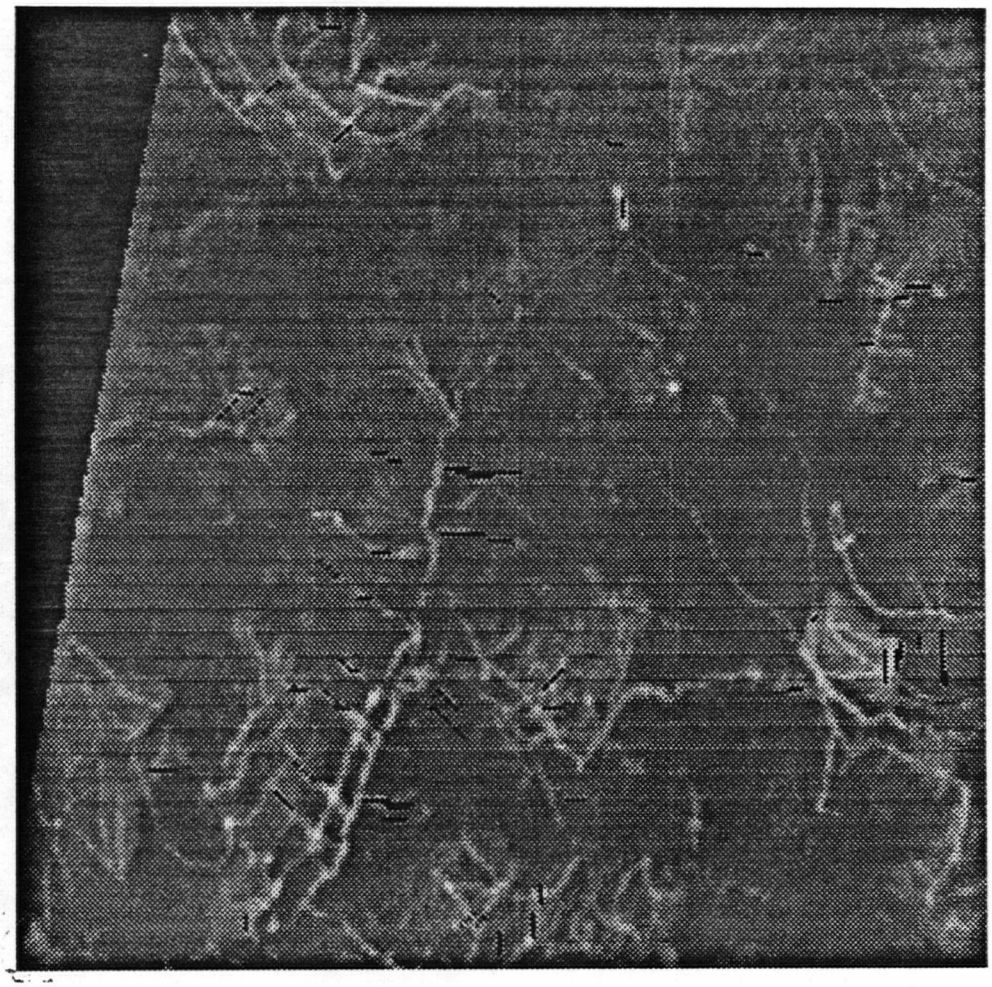

unique commission errors produced by the 5 selected trials, 34 were not clearly explained by photo evidence or were suspected of landslide activity after the inventory was performed. A subsequent field check indicated that 3 of these were landslides which occurred in the interval between inventory and satellite image acquisition, and one was an old, revegetated debris flow. The first 3 were added to the event catalogue for statistical purposes, and the fourth was not added since Howes purposely omitted it. Table 4.2a gives a breakdown of the commission errors that were made, including the harvest condition of the area surrounding the commission. Table 4.2b provides an additional error breakdown in which commission errors are organised by feature origin. Roads and landings are grouped with 'no evidence' and 'other' errors found in recently harvested zones into a 'disturbed' category, while errors due to clearings and ledge are grouped with 'no evidence' and other' errors found in early harvest and old growth zones into a 'natural' category. Figures 4.6 and 4.7 are examples of these errors.

4.1.2 Success characterisation

The landslide attributes extracted from the event catalogue (see Section 2.2.2) were used to examine the identification results. Table 4.3 shows the number of landslides which fall into categories organised from these attributes. These categories will be used to help analyse the results.

Table 4.2a and b. Causes of commission errors. Two breakdowns are presented: (a) specific cause of error, and (b) whether the cause is related to manmade (disturbed) or natural features in the landscape.

Table 4.2a.

Cause	Harvest		Total Number	Percent
	pre-1968	post-1968		
Road or landing	11	16	27	37
No evidence	6	5	11	15
Clearing	7	1	8	11
Ledge or talus	3	3	6	8
Other	6	15	21	29
Total	33	40	73	100

Table 4.2b.

Cause	Harvest		Total Number	Percent
	pre-1968	post-1968		
Natural	22	5	27	37
Disturbed	11	35	46	63
Total	33	40	73	100

Note: The categories for Table 4.2a are outlined in Appendix B. Table 4.2b is described in the text.

Figure 4.6. Commission error A-4. Large, irregular deposits of slash on the landscape were one contributor to commission error.

Figure 4.7. Commission error B-16. Landings, logging scars, and slash were often associated with commission error.

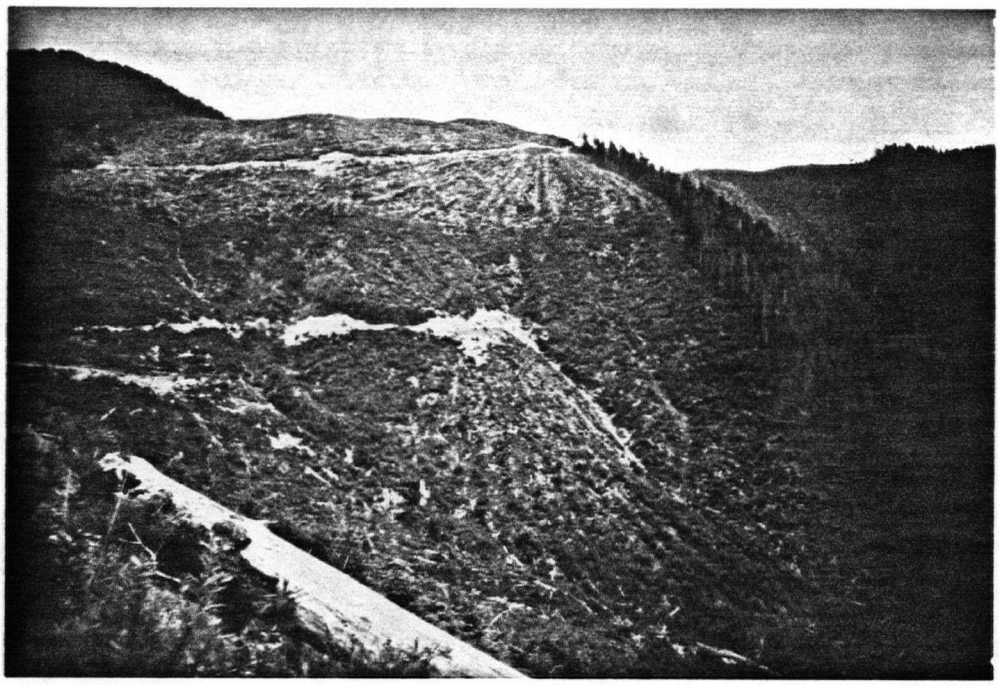

Categorical results for each trial are examined in Tables 4.4 through 4.8. In these tables, four age and harvest conditions are held constant against nine physical characteristics. The four include all events of all ages and all harvest conditions in order to produce an overview. Then all post-1968 events are examined, first in all harvest conditions in Section 2 of the tables, and then in post and pre-1968 harvest conditions in Sections 3 and 4 of the tables. Note that unharvested areas have been grouped with the pre-1968 category, as discussed in Section 2.3.2. Northern and southern aspect locations are considered separately, and are designated by N and S in the tables.

4.2 Discussion

From an operational standpoint, there are unacceptably high commission and omission rates. However, the results compare favourably to those of Gimbarzevsky (1983), where 40% of landslides present in a Landsat MSS scene were detected, because automated interpretation was not used in that study. Because of the range of input parameters (segment length and slope, image threshold) that were used in the trials, no one operator proved to be superior to the others. This is substantiated by Table 4.1, where the three operators appear throughout the table. It seems that all three approaches to image enhancement are equally suited to providing candidate segments for this approach. Other components of the study, such as the method used for object extraction and the type and quality of data available are of

Table 4.3. Total number of events in each landslide category.

Aspect/ Char.	Event Type								
	all events	tor.& flow	slide	long	short	LW	LN	SW	SN
Section 1									
N	72	55	17	42	30	16	26	12	18
S	114	80	34	75	39	29	46	12	27
Section 2									
N	39	29	10	21	18	10	11	8	10
S	59	43	16	38	21	18	20	8	13
Section 3									
N	10	6	4	4	6	0	4	1	5
S	17	12	5	10	7	3	7	3	4
Section 4									
N	29	23	6	17	12	10	7	7	5
S	42	31	11	28	14	15	13	5	9

Section 1: All events considered (total 186).
Section 2: Events occurring after 1968 photos only (total 98).
Section 3: Post-1968 events in an area harvested after 1968 (total 27).
Section 4: Post-1968 events in an area harvested before 1968 or not harvested at all (total 71)

LW- length > 300 m, width > 20m.
LN- length > 300 m, width < 20m.
SW- length < 300 m, width > 20m.
SN- length < 300 m, width < 20m.

Table 4.4. Successful identifications for trial D. All figures are % of total in category

Aspect/ Char.	Event Type								
	all events	tor.& flow	slide	long	short	LW	LN	SW	SN
Section 1									
N	14	11	24	17	30	31	8	17	6
S	20	25	9	25	10	31	22	17	7
Section 2									
N	23	17	40	29	17	50	9	25	10
S	25	33	6	34	10	39	30	13	8
Section 3									
N	10	17	0	25	0	--	25	0	0
S	17	17	17	20	13	33	14	33	0
Section 4									
N	28	17	67	29	25	50	0	29	20
S	29	39	0	39	7	40	38	0	11

Section 1: All events considered (total 186).
Section 2: Events occurring after 1968 photos only (total 98).
Section 3: Post-1968 events in an area harvested after 1968 (total 27).
Section 4: Post-1968 events in an area harvested before 1968 or not harvested at all (total 71)

LW- length > 300 m, width > 20 m.
LN- length > 300 m, width < 20 m.
SW- length < 300 m, width > 20 m.
SN- length < 300 m, width < 20 m.

Table 4.5. Successful identifications for trial M. All figures are % of total in category

Aspect/ Char.	Event Type								
	all events	tor.& flow	slide	long	short	LW	LN	SW	SN
Section 1									
N	14	13	18	17	10	31	8	25	0
S	26	31	12	32	15	38	29	25	11
Section 2									
N	23	21	30	29	17	50	9	38	0
S	29	35	13	34	19	44	25	25	15
Section 3									
N	0	0	0	0	0	--	0	0	0
S	22	25	17	30	13	33	29	33	0
Section 4									
N	31	26	50	35	25	50	14	43	0
S	31	39	9	36	21	47	23	20	22

Section 1: All events considered (total 186).
Section 2: Events occurring after 1968 photos only (total 98).
Section 3: Post-1968 events in an area harvested after 1968 (total 27).
Section 4: Post-1968 events in an area harvested before 1968 or not harvested at all (total 71)

LW- length > 300 m, width > 20m.
LN- length > 300 m, width < 20m.
SW- length < 300 m, width > 20m.
SN- length < 300 m, width < 20m.

Table 4.6. Successful identifications for trial K. All figures are % of total in category

Aspect/ Char.	Event Type								
	all events	tor.& flow	slide	long	short	LW	LN	SW	SN
Section 1									
N	14	11	24	17	10	31	8	17	6
S	31	34	24	29	33	38	24	25	37
Section 2									
N	21	14	40	24	17	50	0	25	10
S	39	44	25	40	48	44	25	25	62
Section 3									
N	0	0	0	0	0	--	0	0	0
S	22	33	0	20	25	33	14	33	25
Section 4									
N	28	17	67	29	25	50	0	29	20
S	45	48	36	39	57	47	31	20	78

Section 1: All events considered (total 186).
Section 2: Events occurring after 1968 photos only (total 98).
Section 3: Post-1968 events in an area harvested after 1968 (total 27).
Section 4: Post-1968 events in an area harvested before 1968 or not harvested at all (total 71)

LW- length > 300 m, width > 20 m.
LN- length > 300 m, width < 20 m.
SW- length < 300 m, width > 20 m.
SN- length < 300 m, width < 20 m.

Table 4.7. Successful identifications for trial N. All figures are % of total in category

Aspect/ Char.	Event Type								
	all events	tor.& flow	slide	long	short	LW	LN	SW	SN
Section 1									
N	19	20	24	26	10	44	15	25	0
S	32	38	21	40	18	45	38	25	15
Section 2									
N	26	24	30	33	17	50	18	38	0
S	36	42	19	45	19	56	35	25	15
Section 3									
N	0	0	0	0	0	--	0	0	0
S	22	25	17	30	13	33	29	33	0
Section 4									
N	34	30	50	41	25	50	29	43	0
S	41	48	18	50	21	60	38	20	22

Section 1: All events considered (total 186).
Section 2: Events occurring after 1968 photos only (total 98).
Section 3: Post-1968 events in an area harvested after 1968 (total 27).
Section 4: Post-1968 events in an area harvested before 1968 or not harvested at all (total 71)

LW- length > 300 m, width > 20m.
LN- length > 300 m, width < 20m.
SW- length < 300 m, width > 20m.
SN- length < 300 m, width < 20m.

Table 4.8. Successful identifications for trial E. All figures are % of total in category

Aspect/ Char.	Event Type								
	all events	tor.& flow	slide	long	short	LW	LN	SW	SN
Section 1									
N	22	20	29	26	17	44	15	25	0
S	29	36	12	37	13	34	40	17	11
Section 2									
N	33	24	50	38	28	60	18	25	10
S	32	40	13	42	14	39	45	13	15
Section 3									
N	20	17	25	0	33	--	0	0	40
S	17	17	17	20	13	33	14	33	0
Section 4									
N	38	30	67	47	25	60	29	29	20
S	38	48	9	50	14	40	62	0	22

Section 1: All events considered (total 186).
Section 2: Events occurring after 1968 photos only (total 98).
Section 3: Post-1968 events in an area harvested after 1968 (total 27).
Section 4: Post-1968 events in an area harvested before 1968 or not harvested at all (total 71)

LW- length > 300 m, width > 20m.
LN- length > 300 m, width < 20m.
SW- length < 300 m, width > 20m.
SN- length < 300 m, width < 20m.

interest in a discussion of this method. Because of the limited scope of this study, the discussion is limited to a review of the observations and the proposal of hypotheses to explain the trial results.

4.2.1 Commission errors

The vast majority of commission errors made by the 5 selected trials were confirmed as errors by photo and field checks. Many (39%) were segments of logging roads or landings. Since roads have the same approximate appearance (low resolution linear object) in the enhanced images as the desired landslide tracks, these commissions are a failure of the DEM portion of the logic. It indicates a coincidence of DEM slope and fall line vector file errors that are either inherent in the data or due to registration problems. The low resolution of the elevation data is a contributing factor. It is uncertain, however, whether the gridding algorithm problem discussed in Chapter 2 had any bearing on these commission errors.

Waste wood on the landscape is another logging feature which contributed to the "no evidence and "other" categories of commission errors. These areas included ridges and gullies where a great deal of slash is present (see Figures 4.8 and 4.9). The presence of waste wood could be an explanation for edges and short segment linears in the enhanced images. These areas are characteristically quite confused in image appearance, with frequent skid trails usually oriented down-

slope and slash forming random patterns on the ground. These patterns likely create candidate objects that are oriented down the fall line. The quality of the DEM data probably has little bearing on this commission error.

Logging features constitute a significant majority of commission errors examined. In Table 4.2b, 63% of the errors from the 5 trials are attributed to man's activities. This result suggests the importance of logging features as the explanation of commission errors. The incidence of these errors would, therefore, decrease significantly if the approach was used in an unharvested areas.

A less important source of error on this site (7%) was due to edges caused by talus and ledge outcrops in the landscape. Because they indicate steep areas and thin soils, they are more likely to be found in unlogged areas. The addition of more contextual information (geology), and a more sophisticated approach to DEM information utilisation (gully locations, segment position on hillslope) could be used to refine the process and reduce this error.

As discussed in Chapter 1, Fischler et al. (1981) developed an approach to combining the results from various edge operators based on the type of error each operator is likely to make. The level of commission error found in each of the trials in this study precluded the use of such a system in this study since there are no "Type I" operators from which to draw so-called "zero cost segments."

4.2.2 Identification successes and omissions

The best overall detection rate for all of the trials was found in Section 4 of Tables 4.4 to 4.8. This segment of the landslide population is therefore of particular interest. This represents the set of more recent landslides which are in old growth forest or areas that were logged previous to 1968. Overall results are consistently greater than the Section 3 breakdown, although a few of the smaller categories deviate from this generalisation. The comparatively small size of the Section 3 categories (all but 2 contain less than 10 members) makes it difficult to draw conclusions. However, one explanation for the above average success in Section 4 is the fact that the more recent landslides are in an early stage of regeneration. This would result in a good spectral contrast with the surrounding forest in the image because of the vegetative and soil exposure contrast. The older surrounding forest causes a better contrast edge than recent clearcuts because the older trees are comparatively dark in this band, and soil exposure in the surrounding forest is minimal.

Landslide geometry seems to be significant in Section 4. Long events are extracted at a higher rate in all but one case (south aspect, trial 3). This is consistent with a greater opportunity for the model conditions to be satisfied in a longer event. Results for process type are less clear, and may reflect the small sample size of slide events. For example, slides on north aspects are consistently detected

at or above the 50th percentile in Section 4. This is a relatively small category (6 events), of which 3 are younger than 1979, and all are characterised subjectively as unvegetated by Howes (1985b). On the south aspect, however, the torrents are detected more often. This is consistent with expectations since the majority of torrents are in the longer category, and that torrents, since they occur in channels, revegetate more slowly than slides because of higher erosion activity.

The characteristics of the omitted events are the opposite of the successes. The size of the omission error suggests improvements are needed to make this approach operational. There is little doubt that the "stairstep" effect encountered in the DEM was not fully solved by the slope operator that was employed. This would contribute substantially to the rejection of landslide image segments. A high accuracy DEM is a prerequisite for a system such as this one which requires fine pixel-to-pixel accuracy. The TRIM project (Terrain Resource Inventory Management) now underway in the BC Ministry of Environment and Parks promises to provide digital elevation for selected areas of the province in an irregular point format suitable for interpolation to a 25 metre grid. Given the high degree of accuracy and quality specified for this project, these data would prove quite valuable for the further investigation of this methodology. For these reasons, this study may be properly considered a preliminary one, with the absolute effectiveness of this

system given better data an open question.

4.2.3. Baseline inventory

There are several problems with the evaluation of the methodology by comparison with this database. The first problem is whether the short category of landslides (<300 m) is defined appropriately. The specified segment lengths in the study (4 and 5 pixels) may be too long to detect the shorter events in the catalogue at some orientations to the grid, and this may prejudice the results downward in this category. Also, because landslides revegetate at differential rates depending on morphologic section (erosion or deposition) (Miles et al., 1984), an event measured from a 1968 photo may present a much shorter edge segment in a 1983 satellite image as the deposition zone revegetates. These facts suggest that the "detectable" catalogue of events in the <300 m category used in this study may be optimistic.

Another issue is the combination of landslides which are less than 100m apart into single "events". The advantage to doing this is that most of the landslides are accounted for, even if it is unlikely that many of them could be discerned as individual landslides because of the low resolution of the imagery. Because of their complex geometry, the low resolution linear object definition was expected to be insufficient to describe these events. However, the results suggest otherwise. The 84 'grouped' events represent 46% of the event catalogue, yet they comprised 50%, 50%, 60%, 53%,

and 47% of the total successful identifications for trials D, M, K, N, and E respectively. Other factors, such as an increased opportunity for the model criteria to be fulfilled in the trials in these larger, more complex features may be an explanation for this outcome.

CHAPTER 5

CONCLUSIONS

5.1. This study

The three edge operators presented in the study provide suitable candidates for low-resolution linear objects in the Landsat TM image. No single operator proved superior to the others. A digital elevation model at a comparable resolution provides valuable input to a reasoning structure for the extraction of landslide features. The implementation of such a structure in this study showed the shortcomings and advantages of such a system.

A model based on a low resolution linear object definition of landslide appearance in three enhanced images and a specific slope and orientation relationship to the DEM was implemented in an automated fashion, and the results were compared to a conventional inventory. The approach was susceptible to commission errors (35% to 75% of identifications for all trials) and identified from 17% to 47% of actual landslides in the landscape. Five trials of the methodology, chosen because of their favourable results with respect to commission errors, were examined in depth to assess the characteristics of their performance.

Results from the five trials of interest ranged from 18% to 28% for successful identifications with a corresponding commission error rate of 35% to 41%. An examination of

these results showed that commission errors would be reduced on sites with less logging activity, and that certain classes of landslides, specifically those in Section 4 of Tables 4.4 to 4.8, representing more recent landslides in older harvest or unharvested areas, were detected at the highest rate. Within this group, longer events (>300 meters) were detected more often than shorter ones. This is particularly true for events which measured wider (>20 metres) on the original inventory map. Torrents were detected more often than slides on south aspects, while the opposite was true on north aspects. However, the sample size for slides on north aspects was quite small (6), rendering the results for this breakdown less meaningful.

These results are disappointing from an operational standpoint, but are comparable with previously reported results for discrimination (not extraction) of slope failure forms in a Landsat image of 40% of those mapped from airphotos (Gimbarzevsky, 1983). Better quality elevation data would provide a better idea of the absolute effectiveness of this approach. The results are more encouraging from a scene segmentation standpoint, as the vast majority of edge image candidate segments were eliminated from each scene. This is demonstrated by a visual comparison of the original enhanced images and their corresponding landslide images.

5.2. Research directions

This study was not an exhaustive consideration of the usefulness of satellite imagery for detecting landslides. An interesting comparison could be made if an experienced photo-interpreter identified the landslides he could see in the image without having previously seen the photos or inventory. Even without the advantage of slope information, the interpreter would invariably produce better results than those seen in this study, because he can interpret scene context.

Scene context, however, may be improved in the edge image of the satellite scene as well. Other low resolution linear objects may be suitable for extraction using similar techniques. For example, streams and roads are also emphasized by the edge operators and have rules regarding their relationship to the elevation model. Streams are always at a low point in a perpendicular transect in the elevation model, while roads obey maximum slope rules. By contrast, hydro-electric lines are persistent linear objects in the image, but have no rules regarding slope or elevation.

A global segmentation of scene linears using these data could assign probabilities to segment assignments that would help to eliminate landslide commissions that are a portion of longer road segments. This type of approach could use a variety of templates or operators with known characteristics regarding specific linear objects in the image. Likelihoods

could be drawn from knowledge about the operator and object shape, geometry, relationship to DEM, and relationship to other linears. This study has shown that this type of approach may provide landslide inventories of a predictable reliability for specific classes of slope failures as well as for mapping other linear objects in the landscape. With the increasing availability of digital elevation data, the accurate segmentation of image features of interest to resource managers will benefit from techniques which successfully integrate this data with imagery.

LITERATURE CITED

Alfoldi, T.T. 1974. Regional study of landsliding in Eastern Ontario by remote sensing. Unpubl. MSc. thesis, Dept of Civil Eng., Univ. of Toronto. 79 pp.

Bailey, R.G. 1972. Landslide hazards related to land use planning in Teton Nat'l Forest. U.S.F.S. Intermountain Region. 131 pp.

Bajcsy, R. and M. Tavakoli. 1973. A computer recognition of bridges, islands, rivers, and lakes from satellite pictures. Proc. Mach. Proc. Conf., Purdue, IN. pp. 54-68.

Bajcsy, R. and M. Tavakoli. 1976. Computer recognition of roads from satellite pictures. 2nd Int'l Conf. on Pattern Recognition.

Ballard, D.H. 1981. Strip trees: A hierarchical representation for curves. Comm. ACM, Vol. 24, No. 5. pp. 310-321.

Colwell, R.N. 1983. Glossary. Manual for Remote Sensing. American Society of Photogrammetry, 16 pp.

Davis, L.S. 1975. A survey of edge detection techniques. Computer Graphics and Image Processing, Vol. 4. pp. 248-270.

Destival, I. and H. LeMen. 1986. Detection of linear networks on satellite images. 8th Int'l conf. on Pattern Recog.

Dishaw, H.E. 1967. Massive landslides. Photogram. Eng., Vol. 32, No. 6. pp. 603-609.

Eliasson, P.T., L.A. Soderblom, and P.S. Chavez, jr. 1981. Extraction of topographic and spectral albedo information from multispectral images. Photogram. Eng. and Rem. Sens. Vol. 48, No. 11. pp. 1571-1579.

Fischler, M.A., J.M. Tenenbaum, and H.C. Wolf. 1981. Detection of roads and linear structures in low resolution aerial imagery using a multisource knowledge integration technique. Computer Graphics and Image Processing, Vol. 15. pp. 201-223.

Gagnon, H. 1975. Remote sensing of landslide hazards on quick clays of Eastern Canada. Proc of the 10th Int'l Symp. Rem. Sens. Env., Ann Arbor, Mich, pp. 803-810.

Gimbarzevsky, P. 1983. Remote sensing of slope failures on the Queen Charlotte Islands. R.N.R.F. Symp. on the Appl. of Rem. Sens. to Res. Mgt., Amer. Soc. Photogram. pp. 409-413.

Gresswell, S., D. Heller, and D.N. Swanston. 1979. Mass movement response to forest management in the Central Oregon Cascades. U.S.F.S. Res. Bull. PNW-84. 26 pp.

Haralick, R.M., S. Wang, and D.B. Elliott. 1981. Spatial reasoning to determine stream network from Landsat imagery. Proc. 6th Int'l Conf. on Pattern Recog. pp. 502-516.

Howes, D.E. 1981. Terrain inventory and geological hazards: Northern Vancouver Island. Assessment and Planning Div. Bull. 5, Terrestrial Studies Branch, B.C. Min. of Env.

Howes, D.E. 1985a. Norrish-Cascade Terrain Map. Cart. Sec., Surveys and Res. Mapping Bran., B.C. Min. of Env. 1 sheet.

Howes, D.E. 1985b. Norrish-Cascade Landslide Inventory Map. Cart. Sec., Surveys and Res. Mapping Bran., B.C. Min. of Env. 1 sheet.

Howes, D.E. 1985c. Norrish-Cascade Clearcut Landslide and Introduced Landslide Debris Rating Map. Cart. Sec., Surveys and Res. Mapping Bran., B.C. Min. of Env. 1 sheet.

Howes, D.E. 1987 (in press). A terrain evaluation method for predicting terrain susceptible to post-logging landslide activity: a case study from the Southern Coast Mountains of British Columbia. B.C. Min. of Env. and Parks. 42 pp.

Johnson, R.B., E.L. Maxwell, and J.A. McKean. 1977. Application of colour density enhancement of aerial photography to the study of slope stability. Proc. 15th Ann. Eng. Geol. Soils Eng. Symp., Idaho State Univ., Pocatello. pp. 199-216.

Majka, M.S. 1982. Reasoning about spatial relationships in the primal sketch. unpubl. MSc. thesis, Dept. of Comp. Sci., Univ of Brit. Col. 85 pp.

Marr, D. and E. Hildreth. 1980. Theory af edge detection. Proc. of the Royal Soc. of London, B-207. pp. 187-217.

McManis, C. 1987. Low-cost image processing. Byte, Vol. 12, No. 3. pp. 191-196.

Miles, D.W.R., F.J. Swanson, and C.T. Youngberg. 1984. Effects of landslide erosion on subsequent Douglas-fir growth and stocking levels in the Western Cascades, Oregon. Soil Sci. Soc. Amer. Jour., Vol. 48. pp. 667-671.

Neilson, T.H. and E.E. Brabb. 1977. Slope-stability studies in the San Francisco Bay region, California. Reviews in Eng. Geol., Vol. 3, Geol. Soc. Amer. pp. 235-243.

Nevatia, R. and K.R. Babu. 1979. Linear feature extraction and description. Proc. of the 6th Int'l Joint Conf. on Artificial Intelligence. pp. 639-641.

O'Loughlin, C.L. 1973. An investigation of the stability of steepland forest soils in the Coast Mountains of S.W. British Columbia. Unpubl. Phd. thesis, Dept. of Forestry, Univ. of Brit. Col. 147 pp.

Pickup, G. and D.J. Nelson. 1984. Use of Landsat radiance parameters to distinguish soil erosion, stability, and deposition in arid Central Australia. Rem. Sens. Env., Vol. 16, No. 3. pp. 195-209.

Poole, D.H. 1969. Slope failure forms; their identification, characteristics and distribution as depicted by selected remote sensor returns. Proc. 6th Int'l Symp. on Rem. Sens. of the Env., Vol II, Ann Arbor, MI. pp. 927-965.

Rib, H.T. 1978. Recognition and identification. in Landslides: Analysis and Control. TRB Special Report 176. pp. 34-80.

Rice, R.M., E.S. Corbett, and R.G. Bailey. 1969. Soil slips related to vegetation, topography, and soils in Southern California. Water Resources Research, Vol. 5. pp. 647-659.

Rice, R.M. and G.T. Foggin. 1971. Effects of high intensity storms on soil slippage in mountainous watersheds in Southern California. Water Resources Research, Vol. 7, No. 6. pp. 1485-1496.

Rollerson, T.P. 1984. Terrain stability study, T.F.L. 44. Land Use Planning Advisory Team, Woodlands Division, Macmillan Bloedel Ltd., Nanaimo, B.C. 86 pp.

Rollerson, T.P. 1987. Personal communication.

Rosenfeld, A. and J.S. Weszka. 1976. Picture recognition. in Digital Pattern Recognition (K.S. Fu, ed.), Comm. and Cyber. Series Vol. 10, Springer-Verlay, N.Y. pp. 135-165.

Shibata, T. 1984. Application of digital terrain model in remote sensing. 7th Int'l Conf. on Pattern Recog. pp. 404-406.

Sondheim, M.W. and R.P. Rollerson. 1985. Quantitative definitions of stability classes as related to post-logging clearcut landslide occurrence. Proc. 9th B.C. Soil Sci. Workshop, B.C. Min. of Env.

Swanson, F.J. and D.N. Swanston. 1977. Complex mass movement terrains in the Western Cascades, Oregon. Reviews Eng. Geol. Vol. 3, pp. 113-124.

Swain, P.H. and S.M. Davis. 1978. Remote Sensing: The Quantitative Approach. McGraw-Hill, N.Y. 396 pp.

Tanguay, M.G. and J.Y. Chagnon. 1972. Thermal I-R imagery at the St. Jean Vianney landslide. Proc. 1st Canadian Symp. on Rem. Sens. pp. 387-402.

Tavakoli, M. and A. Rosenfeld. 1982. Building and road extraction from aerial photographs. I.E.E.E. transactions SMC-12, Jan-Feb. pp. 84-91.

Thomson, B. 1987. Personal communication.

VanDine, D.F. 1985. Debris flows and torrents in the Southern Canadian cordillera. Can. Geotech. Jour., Vol. 22. pp. 44-68.

Varnes, D.J. 1958. Landslide types and processes. in Landslides and Engineering Practice, H.R.B. Spec. Report 29. pp. 20-47.

Varnes, D.J. 1978. Slope movement types and processes. in Landslides: Analysis and Control, T.R.B. Spec. Report 176. pp. 11-33.

Weszka, J.S. 1978. A survey of threshold selection techniques. Comp. Graph. and Image Proc., Vol. 7. pp. 259-265.

Wieczorek, G.F. 1984. Preparing a detailed landslide-inventory map for hazard evaluation and reduction. Bull. of Assoc. of Eng. Geol., Vol. 21, No. 3. pp. 337-342.

GLOSSARY

Affine transform: A linear transformation of one coordinate system into another in order to achieve registration in scale and position between two data sets.

Classification: A mapping based on a decision or set of decisions about the class assignments to an input image based on the measurements taken from a set of image features.

DEM: Digital Elevation Model.

Digital Elevation Model: Elevation measurements of region stored in an image compatible, raster format.

Edge detection: The perception of the presence and location of abrupt changes in gray levels within a digital image.

Gaussian distribution: Analogous to the normal distribution.

Lambertian surface: An ideal, perfectly diffusing surface which reflects energy equally in all directions.

Laplacian: An isotropic, two-dimensional derivative of an image region performed about each discrete image point (pixel).

Low resolution linear object: A linear image region of high brightness values width a depicted width of one to three pixels.

Object extraction: A method for explicitly extracting items from a picture by invoking shape and gray level knowledge about the object. The output of the process is necessarily a mapping of the object's location.

Pattern recognition: The automated process by which unidentified patterns in an image can be classified into a limited number of discrete classes through comparison with other class-defining patterns or characteristics.

Region growing: An approach to object extraction by the addition of points, or the merging of subregions, if appropriate acceptance conditions are satisfied.

Registration: The process of geometrically aligning two or more sets of image data such that resolution elements representing a specific ground area are digitally or visually superimposed.

Segmentation: The division of an image into regions based on a set of criteria.

Template matching: An approach to object extraction in which a set of prototypes for an object class is compared with the image. Areas approximating the prototype according to a set of pre-selected similarity criteria are written to an output image at a distinctive score.

Thematic Mapper: A sensor launched in March, 1984 on Landsat-5 that senses reflected electromagnetic radiation in seven bands at approximately 30 metres resolution (thermal band 120 metres). These bands range from visible blue to thermal infrared.

Thresholding: The segmentation of an image based on a gray level which defines the upper boundary of one class and the lower boundary of another.

TM: Landsat Thematic Mapper.

Tracking: A type of region growing where one begins at a point lying on an edge or curve, and successively accepts neighbouring edge or curve points until the entire object, or the entire curve, has been traversed.

Zero crossings: The contours where the output of an isotropic operator passes through zero.

APPENDIX A

LANDSLIDE DETECTION IN AN ENHANCED SATELLITE IMAGE

Procedure

The Laplacian image described in Chapter 2 was registered to the digital landslide inventory using a three point affine transform. Registration points were in valley locations having approximately the same aspect and elevation. The histogram of this image (Figure 3.8) was used to develop three threshold values for study: pixel value 6, 10, and 14. Photographs were taken of full resolution image quarters on a rendition of the image exported to the MacDonald Dettwiler Meridian (PC) system at the Faculty of Forestry. The images for these photographs were displayed as follows: Laplacian image values above the specified threshold displayed in green at pixel value 100, and the image rendition of the digitised landslide inventory displayed as red at pixel value 100.

Photographic slides of the described images were projected on poster paper, and the locations of the landslides were outlined in red. Although overlap between Laplacian edges and the landslide inventory was expected to be evident by a yellow colour, this effect was hindered by problems with registration in certain portions of the image. Some degree of subjective interpretation was necessary to verify successful detection in these areas.

A simple object definition was employed involving strings of "on" pixels of a certain minimum length. Connected strings of "on" pixels of three or more which coincided with a landslide's estimated location and direction was defined as a success. If a string of two connected "on" pixels was separated from another by one "off" pixel, and this line-up coincided with a landslide location as defined above, this was also considered a success. These successes were recorded on the poster paper and later related to their corresponding event for tabulation of results.

Results and Conclusions

The results are shown graphically in Figures A.1 to A.3. Event detection is considered in terms of two criteria: event type (for events representing landslide groups, the type of the dominant and most recent landslide in that group) and event age (year of first appearance on photography). The total success achieved by the three thresholds is not surprising, and closely parallels an apparent increase in image noise as shown in Figure A.2. It is interesting to note that those events identified as primarily torrents are significantly more detectable than slides, as shown in Figure A.3. This may be due to the smaller sizes common in the slide category, or slower regeneration rates in the torrent tracks. When the detected events are considered in terms of age, as shown in Figure A.4, we see that younger events, which are commonly in an early stage of regeneration (if at all), are detected more often than the

Figure A.1. Results: Detection rate of all landslide events for 3 thresholds of the Laplacian image.

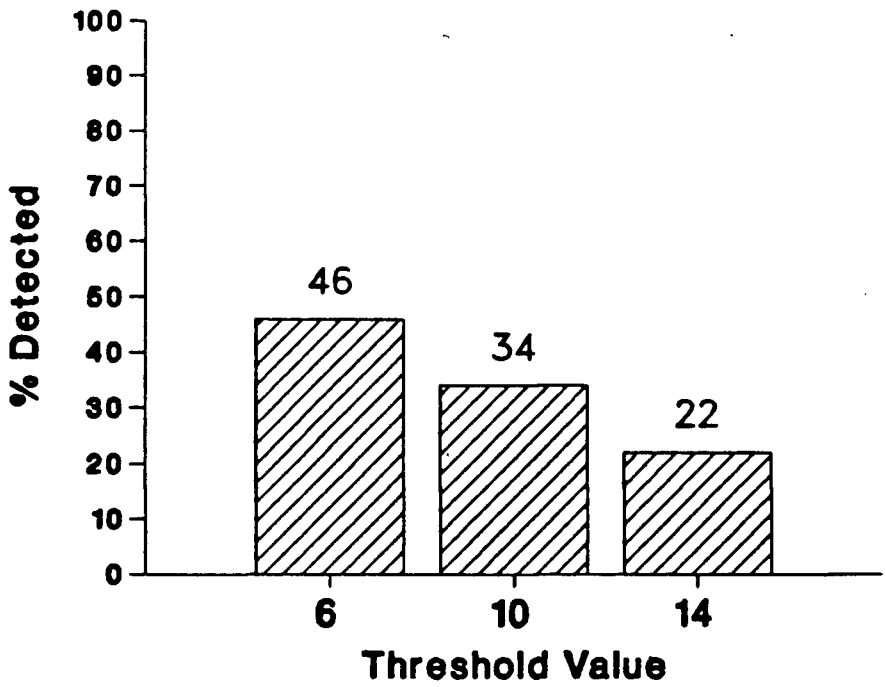

Figure A.2. Results: Detection of landslide events by the Laplacian operator by landslide type.

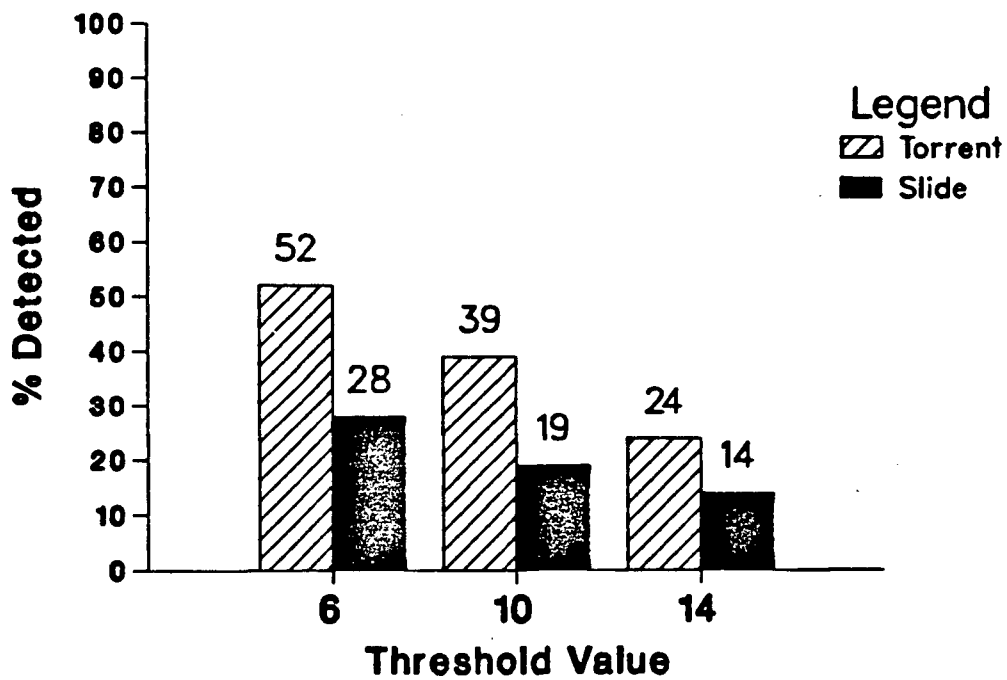

Figure A.3. Results: Detection of landslide events by the Laplacian operator by landslide age.

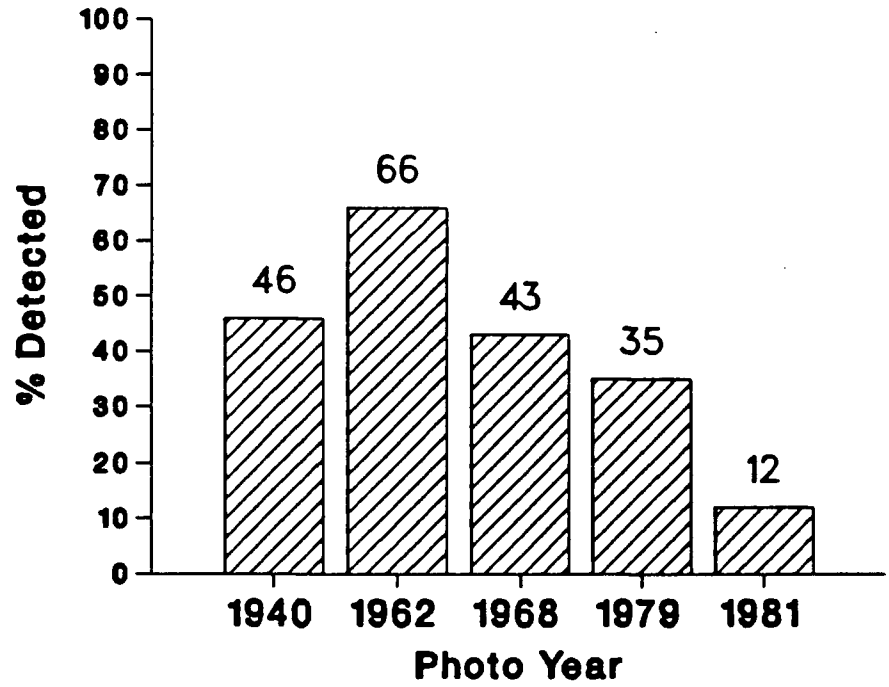

older events.

Two major conclusions were drawn from the results. These conclusions were used to guide the implementation of the thesis. A significant proportion (>50%) of certain classes of events were indicated by this edge operator. These include the combined category of events, events less than 15 years old, and torrents regardless of age which were all detected at or above the 50 percentile in the lowest threshold image. Higher threshold images yielded more disappointing results. However, the low threshold edge image presents a great deal of commission error. Therefore, more informa-

tion, such as the addition of elevation data to a model, is necessary to approach the high level of detection in the low threshold image while reducing the high level of apparent commission. This conclusion should be the same for the template matching and the threshold/template matching images since the world objects which produce all of the low resolution linear objects in these images (i.e. roads, streams, hydroline rights of way) are a constant.

Another conclusion is that the image-to-map registration using the simple 3 point affine transform was found to be unsatisfactory. Therefore, a piecewise approach to registration was employed in thesis to solve local registration problems using this same transformation when registering the elevation data to the images.

This investigation has provided a demonstration of the absolute detectability of landslides using a linear segment definition in an edge-operated image. The results showed that detection was greater than 50% for landslides less than 20 years old, but that the image contained far too much commission error to make this approach suitable for extraction of landslides. Therefore, it was concluded that the addition slope information was necessary for sorting the various candidate segments.

APPENDIX B

RECORD OF COMMISSION ERRORS

These errors were catalogued and their apparent cause documented from photo evidence. Where photo evidence did not indicate the cause, or where there was suspicion of subsequent mass movement, a field check was performed. The description of each column in the table is described below.

1: indicates reference number for segment.

2: indicates harvest condition of surrounding area:

- A: pre-1968 harvest or unharvested.
- B: post-1968 harvest.

3: indicates origin of the error:

- N: error caused by naturally occurring feature.
- D: error caused by feature arising from man's disturbance of the landscape.

4: indicates trials in which the segment occurred.

5: indicates total number of trials in which segment occurred

6: * field check was performed.

7: comments on cause of error.

Appendix B:

			Column Numbers						
1	2	3	4				5	6	7
A 1	A	N	1	2		4	5	4	*	Vegetated gully
A 2	A	N	1		3		5	3		Clearing
A 3	A	N	1		3		5	3		Clearing
A 4	B	D	1					1	*	Gully/slash
A 5	B	D	1		3			2	*	Slash area
A 6	B	D	1		3		5	3	*	Hydroline/road cut
A 7	A	D	1		3		5	3		Road
A 8	A	N	1				5	2	*	No evidence
A 9	A	N	1				5	2	*	No evidence
A 10	B	D	1		3		5	3	*	Gully/slash
A 12	B	D	1	2	3	4	5	5		Hydroline
A 13	A	N		2		4		2	*	No evidence
A 14	A	N		2		4		2		Clearing
A 15	B	D		2		4		2		Road
A 16	B	D		2			5	2		Road
A 17	B	D		2		4		2		Road
A 18	A	D		2		4		2		Road
A 19	A	N		2	3		5	3		Ledge
A 20	B	D		2				1	*	Vegetated gully
A 21	B	D		2		4		2	*	Vegetated gully
A 22	B	N	1	2		4		3	*	Talus slope
A 23	A	N		2	3	4		3		Clearing
A 24	A	D		2	3	4	5	4		Road
A 25	A	N			3			1		Talus slope
A 26	B	D			3			1	*	No evidence
A 27	B	D		2				1		Clearing
A 28	B	D			3		5	2	*	Landing/slash
A 29	A	D			3			1		Road
A 30	A	D			3			1		Landing
A 32	A	N			3			1	*	No evidence
A 34	A	N			3			1		Ledge
A 35	B	D	1		3		5	3		Road
A 36	A	N				4		1		Vegetated gully
A 37	B	N				4		1	*	Ledge
A 38	A	N				4		1		Stream
A 39	B	D				4		1		Hydroline
A 40	A	D				4		1		Road
A 41	A	N				4		1		Stream
A 42	B	D				4		1		Road
A 43	B	N				4		1	*	Ledge
A 44	B	N				4		1		Stream
A 45	A	D			3	4		2		Road
A 46	B	D				4		1		Road
A 47	B	D				4		1	*	Eroded gully
A 48	A	N	1				5	2		Clearing
A 49	B	D					5	1	*	Gully/slash
A 50	B						5	1	*	Torrent
A 51	A	D					5	1		Road
A 52	B	D					5	1	*	No evidence

Appendix B:

Column Numbers

1	2	3	4	5	6	7
A 54	A		5	1	*	Old debris flow
A 55	B		1 2 3 4 5	5		Torrent
B 1	A	N	1	1		Clearing
B 4	B	D	1 5	2	*	Ridge/slash
B 5	B	D	1 5	2		Road
B 6	B	D	1	2		Road
B 7	A		1 3 5	3	*	Slide
B 8	A	D	1 2 4 5	4		Road
B 9	A	N	1	1	*	No evidence
B 10	B	D	2 4 5	3		Road
B 11	A	D	2 4	2		Road
B 12	B	D	2 3 4	3		Road
B 13	A	N	2 4	2		Stream
B 14	B	N	2 4	2	*	Stream
B 15	A	N	2 4 5	3	*	Eroded gully
B 16	B	D	2 4	2		Landing
B 17	B	D	2 4	2		Eroded gully
B 18	B	D	3 5	2	*	Ridge/slash
B 20	A	N	3	1		Clearing
B 21	B	D	3	1	*	No evidence
B 22	B	D	3	1	*	No evidence
B 23	B	D	3	1	*	No evidence
B 24	A	D	3 5	2		Road
B 25	B	D	4	1		Road
B 26	B	D	5	1		Road
B 27	B	D	5	1		Road
B 29	B	D	5	1		Road
B 30	A	N	5	1	*	No evidence

APPENDIX C

EVENT CHARACTERISTICS AND IDENTIFICATION

The events identified from Howes' inventory (Howes, 1985b) are listed and described in the following tables. Three events (204, 300, 301) occurred between the time of the inventory and this study. The table is divided into four sections. Selected columns are described below.

- Number: Event number for reference.
- Description: Howes' landslide identification codes. More than one may be listed for each event.
- Photo year: Photos on which the event's major constituent first appeared.
- Harvest: Photos on which harvesting first became apparent in the area surrounding the event. In the case of multiple harvest years surrounding one event, the primary one is taken.
- Type: S slide, T torrent.
- Operator codes (e.g. T2S20L5):

  T2 image threshold value of 2. o
  S20 minimum segment slope of 20 .
  L5 minimum segment length of 5 pixels.

  1 indicates that the event was extracted by the operation.
  0 indicates that the event was not extracted.

SECTION	NUMBER	DESCRIPTION	PHOTO YEAR	HARVEST TYPE
NW	1	CA-1A -> 1B	68	79 S
NW	2	CA-03	68	62 T
NW	3	CA-06	79	62 T
NW	4	CA-08 -> 09	79	62 T
NW	5	CA-12 -> 13	62	62 T
NW	6	CA-15 -> 19	79	62 T
NW	7	CA-20	81	62 S
NW	8	CA-22	79	62 T
NW	9	CA-24 -> 30	81	62 T
NW	10	CA-36 -> 37	68	62 S
NW	11	CA-39	79	62 S
NW	12	CA-40	79	62 T
NW	13	CA-41	79	62 T
NW	14	CA-42	79	62 T
NW	15	CA-43 -> 45	68	62 T
NW	16	CA-46 -> 46A	79	62 T
NW	17	CA-47	68	62 T
NW	18	CA-65 -> 67	79	68 T
NW	20	CA-68 -> 69	79	68 T
NW	21	CA-70	81	79 T
NW	22	CA-72	79	79 S
NW	23	CA-73	79	62 T
NW	24	CA-73A	81	0 T
NW	25	CA-74 -> 74B	79	62 T
NW	26	CA-77	62	62 T
NW	27	CA-78	79	62 T
NW	28	CA-79 -> 80	79	62 T
NW	29	CA-81	79	0 T
NW	30	CA-82	79	0 T
NW	31	CA-83 -> 85	81	62 T
NW	32	CA-86 -> 87	79	62 T
NW	33	CA-88	79	62 T
NW	34	CA-92 -> 92A	79	62 T
NW	35	CA-94	79	68 T
NW	36	CA-99 -> 100	79	68 T
NW	37	CA-101 -> 104	79	79 T
NW	38	CA-111 ->116	79	68 T
NW	39	CA-117 -> 118	79	68 T
NW	40	CA-119 -> 120	79	79 T
NW	41	CA-121 -> 122	79	0 T
NW	42	CA-121A	79	79 T
NW	43	CA-123 -> 124	81	68 T
NW	44	CA-125	79	68 T
NW	45	CA-126 -> 127	68	68 T
NW	46	CA-128	79	0 T
NW	47	CA-129	79	0 T
NW	49	NR-107	79	79 T
NW	50	NR-108	79	79 T
NW	51	NR-110	62	79 T
NW	52	NR-111	62	79 T
NW	53	NR-112 ->115	62	0 T
NW	54	CC-02 -> 03	40	0 T
NW	55	CC-04 -> 05	40	0 T

SECTION	NUMBER	DESCRIPTION	PHOTO YEAR	HARVEST	TYPE
NW	56	CC-08 -> 12	62	0	T
NW	57	NR-194 -> 198	79	79	T
NW	58	NR-196	79	79	S
NW	59	NR-222 -> 223	79	62	T
NW	60	NR-224	79	62	T
NW	61	NR-225 -> 226	79	62	T
NW	62	NR-228 -> 231	79	62	T
NW	63	NR-205 -> 206	81	62	T
NW	64	NR-207 -> 208	62	62	T
NW	65	NR-209	68	62	S
NW	66	NR-187	62	62	T
NW	67	NR-182 -> 183	79	79	T
NW & NE	68	NR-144 -> 150	62	0	T
NW & SE	70	NR-142	62	0	S
NW & SW	71	NR-132 -> 133	62	0	T
NW	174	CA-10	62	62	T
NW	175	CA-11	62	62	T
NW	176	CA-14	68	62	S
NW	177	CA-32	79	62	F
NW	178	CA-35	79	62	S
NW	179	CA-75 -> 76	79	62	T
NE	72	NR-238 -> 243	68	62	T
NE	73	NR-245	62	62	F
NE	74	NR-250 -> 250A	68	62	T
NE	75	NR-254	81	68	F
NE	76	NR-255	79	62	S
NE	77	NR-256 -> 260	79	68	S
NE	78	NR-262	79	68	T
NE	79	NR-263 -> 266	79	68	T
NE	80	NR-268 -> 268A	79	68	T
NE	81	NR-270 -> 271(273)	62	68	S
NE	82	NR-272	79	68	S
NE	83	NR-275 -> 278	68	62	T
NE	84	NR-279 -> 280	81	62	T
NE	85	NR-217	79	0	F
NE	86	NR-281 -> 282	81	62	T
NE	87	NR-283	81	62	S
NE	88	NR-291 -> 292	62	83	T
NE	89	NR-293 -> 294	62	62	T
NE	90	NR-295 -> 296	62	62	T
NE	91	NR-297	68	62	T
NE	92	NR-298A	81	68	F
NE	93	NR-298 -> 299	81	81	T
NE	94	NR-300	68	62	F
NE	95	NR-302	81	62	T
NE	96	NR-303	81	79	T
NE	97	NR-304	81	62	S
NE	98	NR-306	62	0	S
NE	99	NR-309 -> 311	62	0	T
NE	100	NR-313 -> 317	68	0	T
NE	101	NR-323	62	0	T
NE	102	NR-325	62	0	T
NE	103	NR-326	68	62	S

SECTION	NUMBER	DESCRIPTION	PHOTO YEAR	HARVEST	TYPE
NE	104	NR-328 -> 329	62	0	T
NE	105	NR-331	68	0	T
NE	106	NR-332 -> 333	62	83	T
NE	107	NR-333B -> 333C	62	0	T
NE	108	NR-337	62	0	S
NE	109	NR-347 -> 351	68	0	T
NE	110	NR-355 -> 356	81	81	T
NE	111	NR-178	62	79	T
NE	112	NR-179	62	79	T
NE	113	NR-210 -> 212	81	62	T
NE	114	NR-213 -> 214	81	62	S
NE	115	NR-174	62	0	T
NE	116	NR-151 -> 152	79	68	T
NE	117	NR-154 -> 163	79	79	T
NE	118	NR-164	79	79	S
NE	119	NR-165	79	79	T
NE	120	NR-166	68	79	T
NE	121	NR-167	62	0	S
NE	122	NR-169 -> 170	62	0	T
NE	123	NR-171 -> 171A	68	0	T
NE	124	NR-175	81	62	T
NE	200	NR-168	62	0	T
NE	201	NR-261	81	68	S
NE	202	NR-70	81	83	S
NW	203	CA-01	79	62	S
NW	204	CA-02A	83	62	T
SW	127	WL-09	40	0	F
SW	128	WL-10 -> 11	40	0	F
SW	129	WL-12	40	0	S
SW	130	NR-27 -> 28	40	0	S
SW	131	NR-29 -> 30	40	0	S
SW	132	NR-31	40	0	S
SW	133	NR-32 -> 34	40	0	S
SW	134	NR-48 -> 49 (45)	79	62	S
SW	135	NR-62 -> 63	81	79	S
SW	136	NR-76	79	83	S
SW	137	NR-77 -> 79	81	83	S
SW	138	NR-81	79	83	S
SW	139	NR-84	81	83	F
SW	140	NR-85 -> 86	79	79	T
SW	141	NR-88 -> 89	79	79	T
SW	142	NR-90 -> 91(93,94)	40	79	T
SW	143	NR-92	79	79	S
SW	144	NR-121	62	0	T
SW	145	NR-122 -> 124	68	0	T
SW	146	NR-128 -> 128A	68	0	T
SW	147	NR-129	79	62	T
SW	148	NR-131	62	0	T
SW	149	NR-404 -> 405	68	62	T
SW	150	NR-406	62	62	F
SW	151	NR-412	40	0	S
SW	152	NR-414	40	0	T
SW	153	NR-414A	68	62	S

SECTION	NUMBER	DESCRIPTION	PHOTO YEAR	HARVEST YEAR	TYPE
SW	154	NR-423	40	0	S
SW	155	NR-425 -> 428	68	0	T
SW	156	NR-430	40	0	T
SW	180	NR-65	79	79	S
NE	181	NR-125A	62	0	T
NE	182	NR-127	68	0	T
NE	184	NR-157	62	0	S
SE	157	NR-448 -> 450	81	68	T
SE	158	NR-363 -> 368A	68	62	T
SE	159	NR-372 -> 374	79	79	S
SE	160	NR-375	81	62	S
SE	161	NR-377	62	62	T
SE	162	NR-380	62	62	S
SE	163	NR-381 -> 383(393)	81	62	S
SE	164	NR-387	62	62	T
SE	165	NR-395	68	62	T
SE	166	NR-396	62	62	S
SE	167	DE-01 -> 07	79	79	T
SE	168	DE-08 -> 09	79	79	T
SE	169	DE-11	62	62	S
SE	170	DE-12 -> 13	62	62	S
SE	171	DE-15	62	79	F
SE	172	DE-16	62	79	S
SE	173	DE-21	62	0	T
SE	183	NR-140 -> 141	62	0	T

NO.	ASPECT	LENGTH	WIDTH	L CLASS	W CLASS
1	2	800	10	2	1
2	2	800	40	2	2
3	2	800	60	2	2
4	2	800	40	2	2
5	2	900	20	2	1
6	2	900	40	2	2
7	2	400	40	2	2
8	2	400	20	2	1
9	2	900	30	2	2
10	2	200	20	1	1
11	4	800	60	2	2
12	4	1000	40	2	2
13	4	800	60	2	2
14	4	1000	20	2	1
15	3	500	20	2	1
16	3	800	60	2	2
17	3	800	60	2	2
18	3	500	60	2	2
20	4	700	20	2	1
21	4	200	10	1	1
22	4	200	20	1	1
23	1	400	40	2	2
24	4	150	10	1	1
25	1	500	40	2	2
26	4	400	10	2	1
27	4	400	20	2	1
28	4	600	50	2	2
29	4	200	10	1	1
30	3	600	30	2	2
31	4	200	10	1	1
32	4	500	10	2	1
33	4	300	40	1	2
34	3	600	20	2	1
35	3	500	10	2	1
36	3	800	10	2	1
37	3	400	20	2	1
38	3	600	20	2	1
39	3	800	10	2	1
40	3	700	20	2	1
41	4	300	60	1	2
42	4	500	10	2	1
43	4	300	30	1	2
44	4	300	30	1	2
45	4	200	20	1	1
46	1	500	30	2	2
47	4	300	30	1	2
49	2	900	10	2	1
50	2	1000	10	2	1
51	2	600	10	2	1
52	2	600	10	2	1
53	4	1100	10	2	1
54	3	2200	40	2	2
55	3	400	40	2	2

NO.	ASPECT	LENGTH	WIDTH	L CLASS	W CLASS
56	4	1600	10	2	1
57	2	1000	10	2	1
58	2	200	10	1	1
59	2	200	20	1	1
60	2	500	30	2	2
61	2	300	20	1	1
62	2	900	30	2	2
63	2	800	20	2	1
64	2	800	20	2	1
65	3	200	10	1	1
66	4	800	30	2	2
67	2	300	10	1	1
68	2	1400	20	2	1
70	2	1000	180	2	2
71	2	400	10	2	1
174	2	800	20	2	1
175	2	300	20	1	1
176	2	200	20	1	1
177	2	200	30	1	2
178	2	300	10	1	1
179	4	500	50	2	2
72	3	1000	20	2	1
73	2	300	30	1	2
74	2	800	20	2	1
75	2	400	30	2	2
76	2	600	20	2	1
77	3	1300	30	2	2
78	3	600	20	2	1
79	3	600	20	2	1
80	3	300	20	1	1
81	4	1400	30	2	2
82	3	200	40	1	2
83	3	500	20	2	1
84	4	400	10	2	1
85	1	300	40	1	2
86	4	200	10	1	1
87	4	200	40	1	2
88	3	600	20	2	1
89	3	800	20	2	1
90	3	600	30	2	2
91	2	600	30	2	2
92	2	200	10	1	1
93	3	1000	30	2	2
94	3	150	20	1	1
95	3	400	20	2	1
96	3	200	10	1	1
97	3	400	30	2	2
98	3	1000	10	2	1
99	3	1400	40	2	2
100	4	600	20	2	1
101	3	500	30	2	2
102	1	400	30	2	2
103	1	150	30	1	2

NO.	ASPECT	LENGTH	WIDTH	L CLASS	W CLASS
104	1	400	20	2	1
105	2	600	10	2	1
106	1	600	20	2	1
107	1	1000	10	2	1
108	3	2000	10	2	1
109	4	2400	10	2	1
110	4	400	10	2	1
111	4	300	10	1	1
112	4	800	10	2	1
113	2	1600	40	2	2
114	2	500	50	2	2
115	1	800	20	2	1
116	2	200	20	1	1
117	2	800	20	2	1
118	2	300	30	1	2
119	2	400	30	2	2
120	2	200	10	1	1
121	1	300	30	1	2
122	1	300	10	1	1
123	2	800	10	2	1
124	1	600	10	2	1
200	2	800	10	2	1
201	3	300	20	1	1
202	1	150	20	1	1
203	2	150	20	1	1
204	2	800	40	2	2
127	4	200	10	1	1
128	4	200	50	1	2
129	4	200	80	1	2
130	1	150	30	1	2
131	2	300	50	1	2
132	2	400	30	2	2
133	2	300	30	1	2
134	2	300	30	1	2
135	2	400	40	2	2
136	2	200	10	1	1
137	2	200	20	1	2
138	1	150	30	1	2
139	2	200	30	1	2
140	1	1200	10	2	1
141	2	300	20	1	1
142	1	600	20	2	1
143	1	200	20	1	1
144	3	1000	10	2	1
145	4	200	20	1	1
146	3	200	10	1	1
147	2	300	30	1	2
148	2	400	20	2	1
149	4	200	10	1	1
150	4	200	20	1	1
151	3	200	20	1	1
152	3	500	20	2	1
153	3	200	10	1	1

NO.	ASPECT	LENGTH	WIDTH	L CLASS	W CLASS
154	3	200	30	1	2
155	4	400	30	2	2
156	4	300	20	1	1
180	2	300	50	1	2
181	3	800	10	2	1
182	3	200	10	1	1
184	2	600	10	2	1
157	4	1600	10	2	1
158	3	400	20	2	1
159	4	300	30	1	2
160	1	200	20	1	1
161	4	500	30	2	2
162	4	200	10	1	1
163	4	800	30	2	2
164	4	600	20	2	1
165	4	400	20	2	1
166	4	300	10	1	1
167	1	800	20	2	1
168	2	500	10	2	1
169	2	200	20	1	1
170	2	300	20	1	1
171	2	500	20	2	1
172	2	300	20	1	1
173	3	200	20	1	1
183	2	1100	30	2	2

NO.	T2S20L5	T25S10L4	T3S20L5	T3S20L4	T2S25L5	T3S15L5
1	0	0	1	1	1	1
2	1	1	1	1	1	1
3	1	1	1	1	1	1
4	1	1	1	1	0	1
5	0	1	0	1	0	1
6	1	1	1	1	1	1
7	0	0	0	0	0	0
8	0	1	0	0	0	0
9	0	1	0	1	0	1
10	1	1	1	1	0	1
11	1	1	1	1	1	1
12	0	0	0	0	0	0
13	1	1	1	1	1	1
14	1	1	0	0	0	0
15	1	0	0	0	0	0
16	1	0	1	0	0	1
17	0	1	0	0	0	1
18	0	0	0	1	0	1
20	1	0	0	0	0	0
21	0	0	0	0	0	0
22	0	0	0	0	0	0
23	0	1	0	0	0	1
24	0	0	0	0	0	0
25	1	1	1	1	1	1
26	0	0	0	0	0	0
27	0	0	0	0	0	0
28	1	1	1	1	1	1
29	1	1	1	1	1	1
30	0	0	0	0	0	0
31	0	0	0	0	0	0
32	0	0	0	0	0	0
33	0	1	0	0	0	0
34	0	0	0	0	0	0
35	0	0	0	0	0	1
36	0	1	0	0	0	1
37	1	1	1	1	0	1
38	0	0	0	0	0	0
39	0	1	0	0	0	0
40	0	0	0	0	0	0
41	0	0	0	0	0	0
42	0	0	0	0	0	0
43	0	0	0	0	0	0
44	0	0	0	0	0	0
45	0	0	0	0	0	0
46	1	0	1	1	1	1
47	1	1	1	1	1	1
49	0	0	0	0	0	0
50	0	0	0	0	0	0
51	0	0	0	0	0	1
52	0	0	0	0	0	1
53	0	0	0	0	0	1
54	1	0	0	0	0	0
55	0	0	0	0	0	0

NO.	T2S20L5	T25S10L4	T3S20L5	T3S20L4	T2S25L5	T3S15L5
56	0	0	0	0	0	0
57	1	0	0	1	0	1
58	0	0	0	0	0	0
59	1	1	1	1	1	1
60	1	1	1	1	1	1
61	1	1	1	1	1	1
62	1	1	1	1	1	1
63	0	1	0	0	0	1
64	1	0	1	1	0	1
65	0	0	0	1	0	0
66	0	0	0	0	0	0
67	1	0	0	0	1	0
68	1	0	0	1	1	0
70	0	0	0	0	0	0
71	1	1	0	1	1	1
174	1	0	1	0	0	0
175	1	0	0	0	0	0
176	0	0	0	0	0	0
177	0	0	0	0	0	0
178	0	0	0	0	0	0
179	0	0	0	0	0	0
72	0	1	0	0	0	1
73	0	0	0	0	0	0
74	1	1	1	1	1	1
75	0	0	0	1	0	1
76	0	0	0	0	0	0
77	0	1	0	0	0	0
78	1	0	1	1	0	1
79	1	0	1	1	1	1
80	1	0	1	1	0	1
81	1	1	0	1	1	1
82	0	0	0	1	0	0
83	1	1	1	1	1	1
84	0	0	0	0	0	0
85	1	1	1	1	0	1
86	0	0	0	0	0	0
87	1	1	1	1	1	1
88	0	0	0	0	0	0
89	0	0	0	1	0	1
90	1	0	1	0	0	0
91	1	1	1	1	1	1
92	1	0	0	0	0	0
93	1	1	1	1	0	1
94	1	0	0	0	0	0
95	0	0	0	0	0	0
96	0	0	0	0	0	0
97	0	0	0	1	0	0
98	0	0	0	0	0	0
99	0	0	0	0	0	0
100	0	0	0	0	0	0
101	0	0	0	0	0	0
102	0	0	0	0	0	0
103	0	0	0	0	0	0

NO.	T2S20L5	T25S10L4	T3S20L5	T3S20L4	T2S25L5	T3S15L5
104	0	0	0	0	0	0
105	0	0	0	0	0	0
106	1	0	1	1	1	1
107	1	1	0	0	1	0
108	0	1	0	1	0	1
109	1	0	0	0	0	1
110	0	0	0	0	0	0
111	0	0	0	0	0	1
112	1	0	0	0	0	1
113	0	0	0	0	0	0
114	0	1	0	0	0	1
115	0	0	0	0	0	0
116	1	0	1	0	0	0
117	1	1	0	1	0	0
118	1	1	0	1	1	1
119	0	0	0	0	0	0
120	0	0	0	0	0	0
121	0	0	0	0	0	0
122	0	0	0	0	0	0
123	0	0	0	0	0	0
124	1	1	0	1	1	1
200	1	1	0	1	1	0
201	1	0	1	1	1	1
202	1	0	0	0	0	0
203	1	0	1	1	1	1
204	1	1	1	1	0	1
127	0	0	0	0	0	0
128	0	0	0	0	0	0
129	0	0	0	0	0	0
130	0	0	0	0	0	0
131	1	1	1	1	1	1
132	0	0	0	0	0	0
133	0	0	0	0	0	0
134	1	0	1	1	0	1
135	0	0	0	0	0	0
136	1	0	1	0	0	1
137	1	0	1	1	0	0
138	0	0	0	0	0	0
139	1	0	1	1	1	1
140	0	0	0	1	0	0
141	1	0	1	0	0	0
142	1	1	1	1	0	1
143	0	0	0	1	0	0
144	0	1	0	0	0	0
145	0	0	0	0	0	0
146	0	0	0	0	0	0
147	0	0	0	0	0	0
148	0	1	0	0	0	0
149	0	0	0	0	0	0
150	0	0	0	0	0	0
151	0	0	0	0	0	0
152	0	0	0	0	0	0
153	0	0	0	0	0	0

NO.	T2S20L5	T25S10L4	T3S20L5	T3S20L4	T2S25L5	T3S15L5
154	0	0	0	0	0	0
155	0	0	0	0	0	0
156	0	0	0	0	0	0
180	0	0	0	1	0	1
181	0	0	0	0	0	0
182	0	0	0	0	0	0
184	1	0	0	0	1	0
157	0	0	0	0	0	0
158	1	1	1	1	1	1
159	0	0	0	0	0	0
160	0	0	0	0	0	0
161	0	1	0	1	0	1
162	0	0	0	0	0	0
163	0	0	0	0	0	0
164	0	0	0	0	0	0
165	0	0	0	0	0	0
166	0	0	0	0	0	0
167	0	0	0	0	0	0
168	0	0	0	0	1	0
169	0	0	0	0	0	0
170	1	0	0	1	0	1
171	0	0	0	0	0	0
172	0	1	0	0	0	1
173	0	0	0	0	0	0
183	0	0	0	1	0	0

NO.	T7S20L5	T25S15L4	T7S20L4	T5S25L4	T7S15L5	T5S20L4
1	0	0	1	0	0	1
2	1	1	1	1	1	1
3	1	1	1	1	1	1
4	1	1	1	0	1	1
5	1	1	1	1	1	1
6	1	1	1	1	1	1
7	0	0	0	0	0	0
8	1	1	1	1	1	1
9	0	1	1	0	0	1
10	0	1	1	0	1	1
11	1	1	1	1	1	1
12	0	0	0	0	0	0
13	1	1	1	1	1	1
14	0	0	1	0	0	1
15	0	0	1	0	0	1
16	0	0	1	1	0	1
17	1	1	1	0	1	1
18	0	0	0	0	0	0
20	0	0	1	0	1	1
21	0	0	0	0	0	0
22	0	0	0	0	0	0
23	0	1	0	0	1	0
24	0	0	0	0	0	0
25	1	1	1	1	1	1
26	0	0	0	0	0	0
27	0	0	0	0	0	0
28	1	1	1	1	1	1
29	1	1	1	1	1	1
30	0	0	0	0	0	0
31	0	0	0	0	0	0
32	0	0	0	0	0	0
33	0	1	0	0	0	0
34	0	0	0	0	0	0
35	0	0	0	0	0	0
36	0	1	0	0	1	0
37	1	1	1	0	1	1
38	0	0	0	0	1	0
39	0	0	0	0	0	0
40	0	0	0	0	0	0
41	0	0	0	0	0	0
42	0	0	0	0	0	0
43	0	0	0	0	0	0
44	0	0	0	0	0	0
45	0	0	0	0	0	0
46	1	0	1	1	1	1
47	0	1	0	0	0	0
49	0	0	0	0	0	0
50	0	0	0	0	0	0
51	0	0	0	0	1	0
52	0	0	0	0	1	0
53	0	0	1	0	0	0
54	0	0	0	0	0	0
55	0	0	0	0	0	0

NO.	T7S20L5	T25S15L4	T7S20L4	T5S25L4	T7S15L5	T5S20L4
56	0	0	0	0	0	0
57	0	0	0	1	0	0
58	0	0	0	0	0	0
59	0	1	1	0	0	1
60	1	1	1	0	0	1
61	0	1	1	1	1	1
62	1	1	1	0	1	1
63	1	0	1	1	1	1
64	1	1	1	1	1	1
65	0	0	0	1	0	1
66	0	0	0	0	0	0
67	0	0	0	0	0	0
68	0	0	1	1	0	1
70	0	0	0	0	0	0
71	0	0	1	1	0	0
174	0	0	0	0	0	0
175	0	0	0	0	0	0
176	0	0	0	0	0	0
177	0	0	0	0	0	0
178	0	0	0	0	0	0
179	0	0	0	0	0	0
72	0	0	0	0	0	0
73	0	0	0	0	0	1
74	1	1	1	1	1	1
75	0	0	0	0	1	0
76	0	0	0	0	0	0
77	0	0	0	0	0	0
78	1	0	1	1	1	1
79	1	0	1	0	1	1
80	1	0	1	0	1	1
81	0	0	0	1	0	1
82	0	0	0	0	0	0
83	0	1	1	0	1	1
84	0	0	1	1	0	1
85	1	1	1	0	1	1
86	0	0	0	0	0	0
87	1	1	1	1	1	1
88	0	0	0	0	0	0
89	0	0	0	0	0	1
90	0	0	0	0	0	1
91	1	1	1	1	1	1
92	0	0	1	0	1	1
93	1	1	1	0	1	1
94	0	0	0	0	0	0
95	0	0	0	0	0	0
96	0	0	0	0	0	0
97	0	0	0	0	0	0
98	0	1	0	0	0	0
99	0	0	0	0	0	0
100	0	0	0	0	0	0
101	0	0	0	0	0	0
102	0	0	0	0	0	0
103	0	0	0	0	0	0

NO.	T7S20L5	T25S15L4	T7S20L4	T5S25L4	T7S15L5	T5S20L4
104	0	0	0	0	0	1
105	0	0	0	0	1	0
106	0	0	0	0	0	0
107	0	0	0	0	1	0
108	0	0	0	0	0	0
109	0	0	0	0	0	0
110	0	0	0	0	0	0
111	0	0	0	0	0	0
112	0	0	0	0	0	0
113	0	0	0	0	0	0
114	0	1	0	0	1	0
115	0	0	0	0	0	1
116	0	0	0	0	0	1
117	0	1	1	0	0	1
118	1	1	1	1	1	1
119	0	0	0	0	0	0
120	0	0	0	0	0	0
121	0	0	0	0	0	0
122	0	0	0	0	0	0
123	0	0	0	0	0	0
124	0	1	1	1	1	1
200	0	1	1	1	0	1
201	0	0	0	1	0	0
202	0	0	1	0	1	1
203	0	0	0	0	0	1
204	1	1	1	0	1	1
127	0	0	0	0	0	0
128	0	0	0	0	0	1
129	0	0	0	0	0	0
130	0	0	0	0	0	0
131	1	1	1	1	1	1
132	0	0	0	0	0	0
133	0	0	0	0	0	0
134	0	0	0	0	0	0
135	0	0	0	0	0	0
136	0	0	0	0	0	0
137	0	0	0	0	0	0
138	0	0	0	0	0	0
139	0	0	1	1	0	1
140	1	0	1	1	0	1
141	0	0	0	0	0	0
142	1	1	1	0	1	1
143	0	0	0	0	0	0
144	0	0	0	0	0	0
145	0	0	0	0	0	0
146	0	0	0	0	0	0
147	0	0	0	0	0	0
148	1	1	1	1	1	1
149	0	0	0	0	0	0
150	0	0	0	0	0	0
151	0	0	0	0	0	0
152	0	0	0	0	0	0
153	0	0	0	0	0	1

NO.	T7S20L5	T25S15L4	T7S20L4	T5S25L4	T7S15L5	T5S20L4
154	0	0	0	0	0	0
155	0	0	0	0	0	0
156	0	0	0	0	0	0
180	0	0	0	0	0	0
181	0	0	0	0	0	0
182	0	0	0	0	0	0
184	0	0	1	1	0	1
157	0	0	0	0	0	1
158	0	1	0	0	1	1
159	0	0	0	0	0	0
160	0	0	0	0	0	0
161	0	0	0	0	1	1
162	0	0	0	0	0	0
163	0	0	0	0	0	0
164	0	0	0	0	0	1
165	0	0	0	0	0	0
166	0	0	0	0	0	0
167	0	0	1	1	0	0
168	0	0	0	0	0	0
169	0	0	1	0	0	1
170	0	0	0	0	0	0
171	0	0	0	0	1	0
172	0	1	0	0	0	0
173	0	0	0	0	0	0
183	0	0	1	0	0	0

APPENDIX D

LANDSLIDE TEMPLATE REVISION

An oversight was discovered in the configuration of the landslide template after the study was completed. The four directions examined in the template (see Figure 2.6) are insufficient for detecting certain object termini. All eight pixels surrounding the centre should be considered in order to make a rigorous examination of these objects.

A preliminary investigation of the effectiveness of this revised approach was made. The resulting enhanced images from the template/image and template/threshold operations were remarkably similar to those used in the study. Five trials, two using the template/image and three using the template/threshold approaches, were made. The trials were examined for number of successful identifications and commission errors, and the results tabulated with the study results in Table D.1. They are indicated by the double letter symbols.

The results are comparable, and indicate some improvement in landslides detected for identical trials with the original template images, especially in the template/threshold approach. However, an increase in both successful identifications was accompanied by an increase in commission errors. This is consistent with the results from the enhanced images used in the study, which indicates the persistence of commission errors in this approach to object

extraction. It also suggests that the study template, though not ideal, provides suitable candidate objects for this system. Succeeding studies are advised to use the eight direction template.

Table D.1. Success and commission results for study trials plus the revised, eight direction template.

Rank by Commission	Rank by Success	Trial	Operator	Success %	Success No.	Commission %	Commission No.
1	19	D	Laplacian	18	33	35	18
2	15	M	thr./temp4.	23	42	35	23
3	13	K	template4	24	45	37	26
4	14	BA	template8	24	44	37	26
5	9	N	thr./temp.	28	51	41	35
6	8	E	Laplacian	28	51	41	36
7	10	BB	thr./temp8.	25	46	42	34
8	3	BC	thr./temp8.	36	67	45	55
9	16	BD	template8	20	38	48	35
10	17	I	template4	19	36	49	34
11	4	J	template4	36	67	49	65
12	7	F	Laplacian	31	57	50	56
13	12	C	Laplacian	24	45	51	47
14	5	H	template4	36	66	53	73
15	6	L	template4	34	62	55	76
16	11	BE	template8	24	45	63	64
17	1	G	template4	48	89	62	147
18	2	B	Laplacian	37	68	70	158
19	17	A	Laplacian	19	35	70	83

Definitions:

Template4 - original, four direction template used in study.

Thr./temp4. - four direction template used on four thresholds and the results summed.

Template8 - eight direction template.

Thr./temp8. - eight direction template used on four thresholds and the results summed.

Trial BA - minimum slope 15^{o}, minimum length 5 pixels
Trial BB - minimum slope 20^{o}, minimum length 4 pixels
Trial BC - minimum slope 15^{o}, minimum length 4 pixels
Trial BD - minimum gray level 4, minimum slope 20^{o}, minimum length 5 pixels
Trial BE - minimum gray level 3, minimum slope 20^{o}, minimum length 5 pixels

Other trial references are in Table 3.1.